Kim *et al. Soft Sci* 2024;4:24
DOI: 10.20517/ss.2024.09

Soft Science

Review Article

Open Access

Check for updates

Body-attachable multifunctional electronic skins for bio-signal monitoring and therapeutic applications

Kang Hyeon Kim[1,2], Jeong Hyeon Kim[1,3], Yu Jin Ko[1], Han Eol Lee[1,2,3,*]

[1]Division of Advanced Materials Engineering, Jeonbuk National University, Jeonju-si 54896, Republic of Korea.
[2]Division of Electronics and Information Engineering, Jeonbuk National University, Jeonju-si 54896, Republic of Korea.
[3]Department of JBNU-KIST Industry-Academia Convergence Research, Jeonbuk National University, Jeonju-si 54896, Republic of Korea.

[*]**Correspondence to:** Prof. Han Eol Lee, Division of Advanced Materials Engineering, Jeonbuk National University, 567 Baekje-Daero, Deokjin-gu, Jeonju-si 54896, Republic of Korea. E-mail: haneol@jbnu.ac.kr

How to cite this article: Kim KH, Kim JH, Ko YJ, Lee HE. Body-attachable multifunctional electronic skins for bio-signal monitoring and therapeutic applications. *Soft Sci* 2024;4:24. https://dx.doi.org/10.20517/ss.2024.09

Received: 11 Mar 2024 **First Decision:** 17 Apr 2024 **Revised:** 20 May 2024 **Accepted:** 23 May 2024 **Published:** 12 Jun 2024

Academic Editors: Sang Min Won, Xinge YU **Copy Editor:** Dong-Li Li **Production Editor:** Dong-Li Li

Abstract

The lack of infrastructure and accessibility in medical treatments has been considered as a global chronic issue since the concept of treatment and prevention was presented. After the COVID-19 pandemic, the medical reaction capability for epidemic outbreak/spread has been spotlighted as a critical issue to the fore worldwide. To reduce the burden on the medical system from the simultaneous disease emergence, the personalized wearable electronic systems have arisen as the next-generation biomedical monitoring/treating equipment for infectious diseases at the initial stage. In particular, electronic skin (e-skin) with its potential for multifunctional extendibility has been enabled to be applied to next-generation long-term healthcare devices with real-time biosignal sensing. Here, we introduce the recent enhancements of various e-skin systems for healthcare applications in terms of material types and device structures, including sensor components, biological signal sensing mechanisms, applicable technological advancements, and medical utilization.

Keywords: Multifunctional devices, wearable devices, electronic skins, bio-signal monitoring, healthcare application

INTRODUCTION

In modern society, with the convergence of humans and technology, body-attachable electronic devices have attracted much attention as a core technology with the potential to make a breakthrough in various

fields. These devices offer a new interaction paradigm and hold the potential to revolutionize healthcare/treatment by continuously monitoring and analyzing human vital signs in real time[1]. By directly attaching the device onto the skin, it accurately measures diverse vital signs such as heart rate, blood pressure, blood sugar, electromyography, and body temperature, enabling early diagnosis, prevention, and treatment of diseases. It can also effectively manage chronic disease by continuously monitoring personal health status and providing personalized healthcare solutions[2,3]. For example, it can support appropriate insulin administration by real-time monitoring blood sugar levels in diabetic patients and detect and treat arrhythmias by analyzing electrocardiograms in patients with heart disease. These techniques have been very useful in understanding diseases and the various mechanisms behind them. However, patients suffering from chronic diseases and potentially fatal symptoms still face limited accessibility to medical treatment and monitoring. Those with chronic diseases require real-time monitoring of bio-signals throughout their lifetime, such as pulse, blood pressure, and glucose levels. Additionally, new diseases continue to emerge over the years, increasing the number of patients. The complexity of patient diagnoses increases the demand for medical personnel and infrastructure. These comprehensive demands on medical services and personal healthcare for patients and potential patients have exponentially increased in the last several decades[4].

In particular, the COVID-19 pandemic led to the rise of wearable sensors for individual consuming applications for the long-term health monitoring platforms and early-stage response systems for medical diagnostics[5]. Recently, several research groups have made efforts to simultaneously monitor multiple bio-signals with attachments to the human body for the accurate diagnosis of diseases, which are expressed by various and complex symptoms[6]. Therefore, it is important to develop wearable sensors with the selectivity and high sensitivity required for each physical factor (e.g., mass, displacement, temperature, and voltage difference)[7].

In terms of materials, organic materials have the crucial advantage of inexpensive/simple fabrication processes, increasing the mass-production possibility of the realized sensor devices[8]. Despite their complex fabrication procedures and high-temperature requirements, inorganic sensing materials (e.g., compound semiconductors, metal oxides, and nanomaterials) have acquired significant attention due to their higher sensitivity, lower power consumption, and longer lifetimes compared to organic sensing materials[9,10]. Therefore, studies have been actively conducted to implement sensors with improved performances by solving the shortcomings of each material or complementing the existing limitations in a hybrid form[11,12].

Numerous researchers have proposed innovative device structures, such as large-scale arrays, three-dimensional (3D) stacking, and heterogeneous integration, to overcome the physical and structural limitations of conventional devices[13]. Thanks to the dedicated efforts of researchers and the progressions in state-of-the-art wearable sensors, biomedical research has significantly advanced to achieve remarkable accuracy in detecting various organ bio-signals, such as skin strain, ions in sweat, and photoplethysmography (PPG)[14].

Electronic skin (e-skin) is defined as an artificial skin system with sensory capabilities, such as sense of strain, pressure, and temperature, to target complete imitation of human skin sensation. For example, in order to mimic the sense of touch, the e-skin needs to consist of highly sensitive flexible electronic sensors with superior resolution for achieving realistic recognition. By integrating the sensors with a signal transmitting module, the e-skin enables the transfer of its electrical signal to machinery, skin-attachable wearable systems, and man-machine interaction devices.

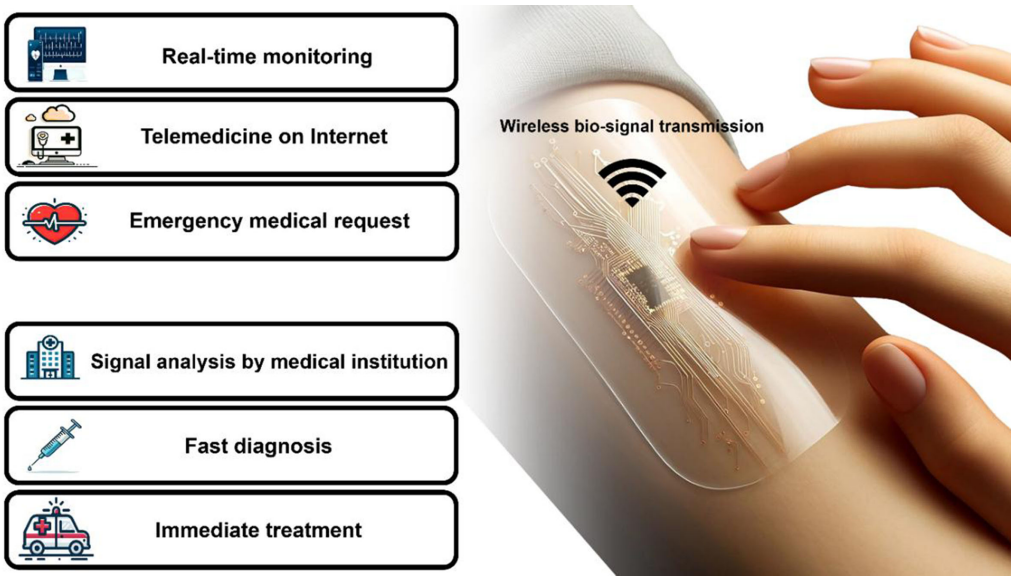

Figure 1. Schematic illustration of skin-attachable multifunctional electronics for personal healthcare.

E-skin has attracted attention with some special advantages such as small device size, lightweight, and conformal attachment onto the skin surface compared to the conventional bulk sensing devices[15]. Moreover, the e-skin system can be easily integrated with additional features including biodegradable materials, wireless power generators, and medicine actuators[16]. With this significant expandability, the e-skins combined with novel sensors are predicted to open up the commercialization of multifunctional medical devices that play a crucial role in real-time biomedical monitoring.

The e-skin systems with various bio-signal sensors enhance the personal healthcare platforms of users. These systems collect various bio-signals in real time, such as heart rate, blood pressure, saliva, and sweat, which are easily influenced by physical and psychological states[17]. By wirelessly transmitting/receiving this data between the users and the medical institution, the individual medical records are easily shared with healthcare professionals, utilized for tracking disease causes, conducting medical research, and gathering diagnostic information more efficiently than before[18]. The recently developed e-skins with bio-signal sensors enable faster and more accurate diagnoses than conventional telemedicine systems. Throughout the COVID-19 pandemic, telemedicine emerged as a major alternative in the healthcare system because this system played a critical role in providing accessible medical assistance to patients unable to reach medical facilities easily[19]. However, the conventional remote medical services often resulted in misdiagnoses compared to in-person examinations due to reliance on fragmented symptoms and inaccurate explanations from the patients[20]. For instance, serious conditions such as cancers can be misdiagnosed as simple illnesses such as colds or indigestion due to insufficient medical information. Since the accurate diagnoses to patients are especially important to not miss the timing for appropriate medical treatments, developing the e-skin system with vital sensing functions is required.

Here, we introduce the overall development strategy of multifunctional e-skins for wearable healthcare applications. In particular, we concentrate on multifunctional and flexible sensing devices and their recent research advancements to achieve these goals. At first, we focus on how individual patients can use e-skin to diagnose, monitor, and treat disease. Next, this review is classified into three major categories to explain the recent research progress: (i) unit sensing components including strain/pressure sensors and optoelectronic sensors; (ii) important features applicable in wearable sensor systems; and (iii) practical healthcare applications.

Electronic skin and healthcare applications

Organ-attached e-skin systems are strategically applied to monitor significant bio-signals for personal healthcare [Figure 1]. These systems collect bio-signals from the equipped sensors and then convert them into personal medical data. This data is wirelessly transmitted to various medical services including real-time health monitoring, internet network-based telemedicine for fast disease diagnosis, and emergency medical alerts for acute diseases[21,22]. For example, when the cardiovascular patients are in an acute heart attack, the following order is carried out in a series: (i) the e-skin systems, which have been continuously monitoring the heart rate, transmit the recorded information thus far to a nearby medical institution; (ii) Medical team checks the biosignals of heart rate, saturation of partial pressure oxygen (SpO_2) level and blood pressure and (iii) sends the medical alert to caregivers and emergency services. This process is not only limited to cardiovascular patients but is also critical to other patients requiring real-time vital sign monitoring.

Figure 2 provides a concise overview of the essential factors for realizing multifunctional and flexible sensing devices, including e-skin components, integrated sensing devices, bio-signal sensing applications, and their medical applications. Since the components of skin-attached e-skins should be soft enough to withstand mechanical stress from the physical movement of the human body, the fabrication processes for flexible and stretchable devices have been actively developed. To apply the device to the e-skin as a component, flexible photodetectors (PDs) have been realized with polymer composite materials, organic materials, and p-n junction semiconductors[23]. Micro-scale light-emitting diodes (μLEDs) have been manufactured to earn flexibility for integration with wearable substrates[24]. Nevertheless, these miniaturized unit devices can only detect a single signal in a limited small surface region with low sensing reliability. To overcome this issue, the integrated circuit array has great merit in multifunctional devices with large-scale sensing, efficient power consumption, and reduced manufacturing costs[25].

For reliable bio-signal sensing, although commercial 'smart watches' have been commercialized with sensing features (e.g., PPG, stress score, and nighttime sleep patterns), the intrinsic gap between these devices and human skin can result in inaccurate vital levels or limited accessibility[26,27]. Skin-adhesive devices, which can be conformally attached onto the human skin surface, have recently risen in popularity for providing more precise bio-signal sensing data, as they can send more health vital signals than conventional devices[28]. In particular, the sensing accuracy of e-skin has been enhanced due to advancements in materials engineering and fabrication processes, enabling the application of e-skin systems with several sensors and actuators in the medical field. For example, these systems regulate therapeutic actuation in real-time such as administering medication, providing heat transfer treatments, delivering electrical stimulation, and drug delivery systems (DDSs), all accomplished by signal information from sensors adhered to the skin[29-31]. Recently, the closed-loop systems with the microneedle-based chemical sensors and drug delivery devices have been designed for accurate drug dose control with immediate feedback. Microneedle arrays enabled the detection of the ion concentration in the interstitial fluid and the control of the DDS for the glucose level monitoring and sustenance of diabetic patients[32,33]. Although these systems were originally designed for diabetes management, they have been applied to overcome several other illness models, such as seizures, stroke, and aneurysms, in recent years.

UNIT SENSING COMPONENTS

Piezoelectric and capacitance-based mechanical sensors

Strain sensors are considered as a crucial requisite for skin-attachable devices because the skin, the largest

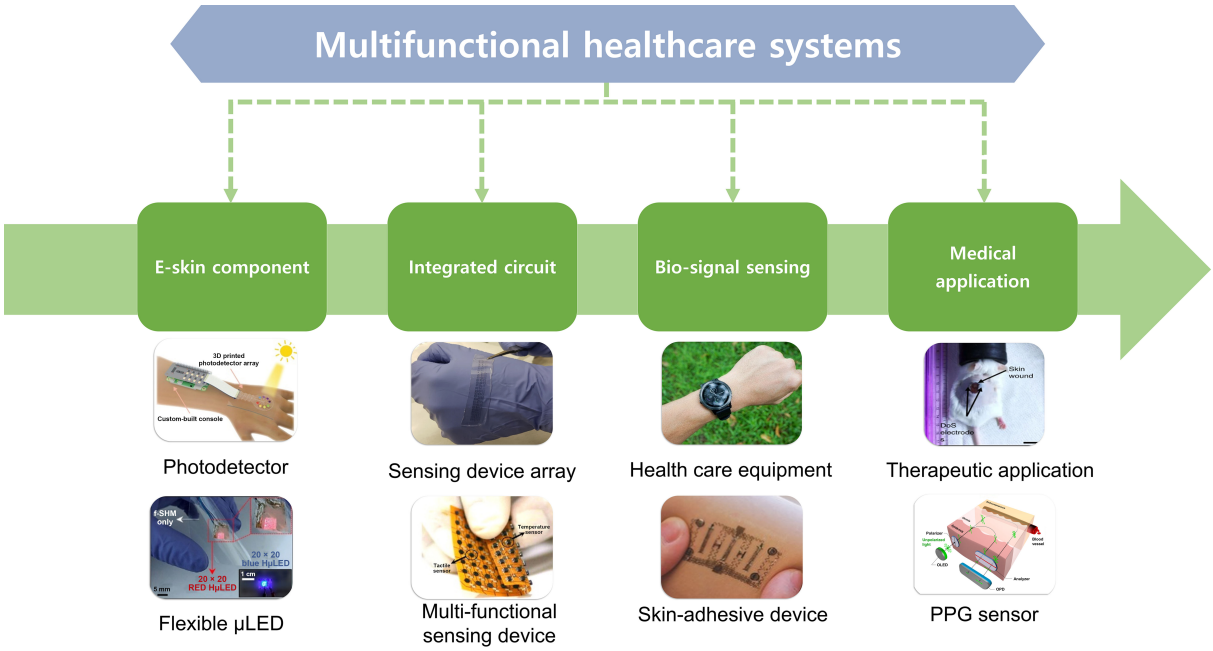

Figure 2. Developing sequence of multifunctional e-skins for biomedical applications. Figure "Photodetector" Reproduced with permission from ref[23]. Copyright 2022, John Wiley and Sons; Figure "Flexible μLED" Reproduced with permission from ref[24]. Copyright 2022, American Chemical Society; Figure "Sensing device array" Reproduced with permission from ref[25]. Copyright 2019, Springer Nature; Figure "Multi-functional sensing device" Reproduced with permission from ref[26]. Copyright 2007, Elsevier; Figure "Skin-adhesive device" Reproduced with permission from ref[27]. Copyright 2016, Elsevier. Figure "Therapeutic application" Reproduced with permission from ref[28]. Copyright 2020, Springer Nature; Figure "PPG sensor" Reproduced with permission from ref[29]. Copyright 2022, AAAS. μLED: Micro-scale light-emitting diode; PPG: photoplethysmography.

organ in the human body, continuously receives various forms of mechanical strains (e.g., bending, stretching, compressing, and twisting) during everyday movements. Wearable strain sensors are usually divided into three main categories based on their working principles: piezoresistive, capacitive, and piezoelectric effects [Figure 3A][34]. Piezoresistive type sensors comprise conductive or semiconductor layers between two electrodes and transform the applied force into a resistance signal. The resistance (R) in resistive type pressure sensor is expressed as follows:

$$R = \frac{\rho L}{A} \tag{1}$$

where ρ is the resistivity, L is the length, and A is the contact area with the electrode. Generally, contact area/resistivity values are constant, and the length of the active layer is the only variant of resistance determined by applied force. The only difference between capacitive and piezoelectric type sensors is an active layer with dielectric and piezoelectric materials. Capacitance C of the capacitive type sensors is conformed to the capacitance of parallel plate capacitors calculated by:

$$C = \frac{\varepsilon A}{d} \tag{2}$$

where ε represents the dielectric constant, A is the electrode-active layer overlapping area, and d is the interval between two plates. With the same active layer material, interval length changes of the two

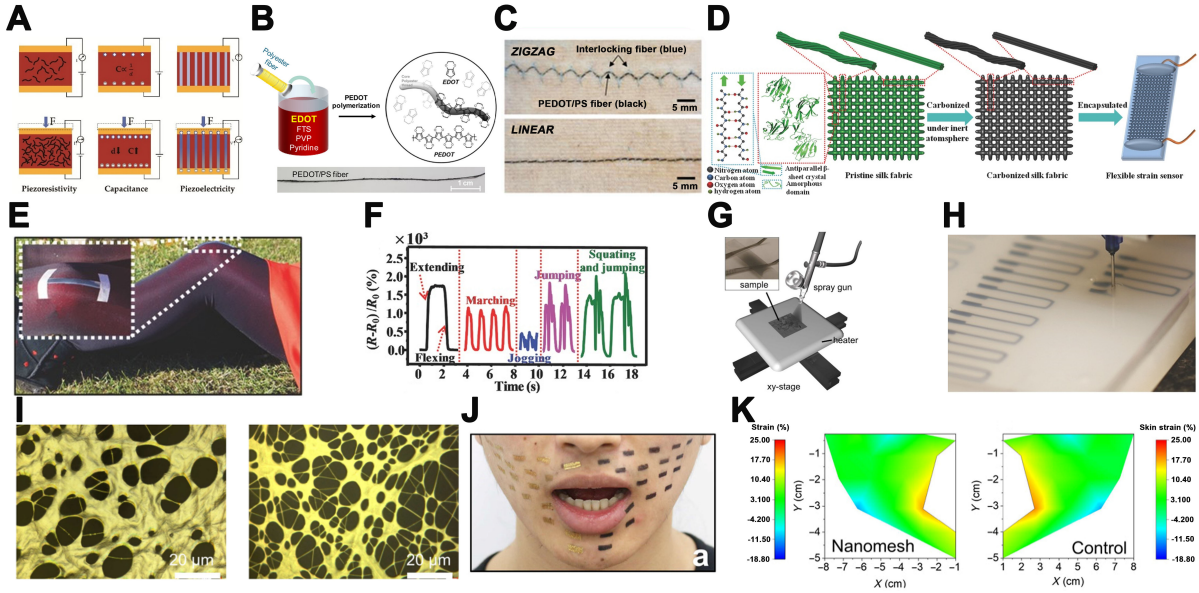

Figure 3. Fabrication process and signal measurements of piezoelectric and capacitance-based mechanical strain sensors. (A) Schematic illustrations of mechanical sensor operating mechanisms: piezo-resistivity, capacitance, and piezoelectricity. Reprinted with permission from ref[34]. Copyright 2020, Elsevier; (B) Fabrication method of PEDOT on a PS fiber for realizing textile sensors; (C) Optical images of linear- and zigzag-type textile strain sensors embedded in fabrics. Reproduced with permission from ref[36]. Copyright 2017, American Chemical Society; (D) 3D images of the CSF strain sensor fabrication; (E) Photograph of the wearable sensors weaved into a stocking. The inset is a magnified image; (F) Resistance changes graph of the wearable sensor at the movements of flexing/extending, marching, jogging, jumping, and squatting-jumping. Reproduced with permission from ref[37]. Copyright 2016, John Wiley and Sons; (G) Schematic of experimental setup for fabricating the flexible strain gauge through the spraying process. Reproduced with permission from ref[39]. Copyright 2022, American Chemical Society; (H) Photograph of e-3DP for a planar array of soft strain sensors. Reproduced with permission from ref[40]. Copyright 2014, John Wiley and Sons; (I) Microscopic images of the PDMS/hexane nanomesh with various weight ratios 1/40 (left) and 1/80 (right); (J) Photograph of nanomesh based-sensor (left side) and control device array (right side) attached on the face during speech of "a" (K) Strain distribution images during speech of "a" with nanomesh-based sensor (left) and control one (right). Reproduced with permission from ref[41]. Copyright 2020, AAAS. PEDOT: Poly(3,4-ethylenedioxythiophene); PS: polyester; 3D: three-dimensional; CSF: carbonized silk fabric; e-3DP: embedded 3D printing; PDMS: polydimethylsiloxane.

electrodes only affect the capacitance difference which measures the pressure to electrical capacitance difference. Piezoelectric materials generate deformation in a certain direction by external force to electricity. Polarization of sensitive material creates the positive and negative charges to different surfaces, forming a potential difference enhanced by external force[35].

In particular, organic materials have been extensively studied for flexible piezoresistive and capacitive sensors because of their simple fabrication process, mechanical stability, easy scalability, and applicability to versatile substrates. Figure 3B and C shows textile strain sensors enabled by polymerized conductive poly(3,4-ethylenedioxythiophene) (PEDOT)-coated polystyrene (PS) fibers[36]. The PEDOT/PS-based strain sensor exhibited excellent identification capabilities for physical states, resulting in a $\Delta R/R_0$ of ~20% at a knee angle difference of approximately 90°. This lightweight and ultrathin PEDOT/PS strain sensor had a superior strain gauge factor (GF) of over 0.76, easily integrating with conventional clothes. Combined with a user-interface (UI) device, the device distinguished hand gestures and translated sign language into letters.

Wang *et al.* demonstrated a highly stretchable and stable carbonized silk fabric (CSF)-based strain sensor with a 9.6 GF under 250% strain and 37.5 GF from 250% to 500% strain, enduring > 500% stretching strain[37]. Figure 3D illustrates a fabrication schematic of the CSF textile, which was thermally carbonized under an Ar-rich atmosphere and encapsulated by elastic silicone (Ecoflex). This CSF textile-based strain

sensor was stably integrated with clothing such as gloves and stockings, detecting various human motions [Figure 3E]. The CSF-based device monitored and specified knee joint motions such as extending/flexing, marching, jogging, jumping, and combinations of squatting/jumping [Figure 3F]. The results from the carbonated silk-based strain sensors suggest that textile devices can be easily and simply produced using other fabrics including wool, cotton, and other artificial fiber fabrics.

With the increased demand for mass production of strain sensors, several research teams have explored cost-effective and scalable production methods using the fluidic properties of organic materials, such as spraying, ink-jet printing, and 3D printing techniques[38]. Among these methods, printing-on-substrate techniques, including 3D printing and ink-jet printing, promise advances in high resolution, sophisticated structure manufacturing, and mass production. Figure 3G displays a schematic illustration of a flexible strain gauge utilizing a 2D material-percolated thin film, realized by spraying a graphene flake-distributed 1-methylpyrrolidone (NMP) solution and instantly annealing it[39]. The applied strain degree was evaluated by measuring the resistance change caused by the conduction pathway breakdown of graphene flakes in the thin film. The sensitivity of the graphene flake network-based device was reliable under various strain values and easily modulated by tuning the 2D material ratio in the sprayed solution. The solution spraying-on-substrate method has the potential for commercializing wearable strain sensors using other 2D materials with low-cost production and easy scalability.

Figure 3H is a process image of an embedded 3D printing (e-3DP) method on elastomeric matrices using ink-form sensing materials, enhancing the stretchability and tunability of the active material by controlling the printing path. Muth *et al.* printed carbon conductive ink at the interface between Ecoflex and silicone thinner to demonstrate highly conformal and extensible elastomeric electronics[40]. The printing parameters, including nozzle size, pressure, and printing speed, were sophisticatedly optimized to realize the specific shape "hairpin". The resistance of the printed ink increased from 11 to 60 kΩ by decreasing the cross-sectional areas of the features (0.71 to 0.066 mm^2) with the printing speed increase. Furthermore, the structure and electrical properties of the conductive ink were stably maintained on the cured elastomer under stretching/bending conditions.

Wang *et al.* reported an ultrathin, mechanically stable, and durable nanomesh-based strain gauge enabled by an electrospinning and dipping process of polyurethane (PU) nanomesh conductors[41]. Figure 3I indicates the fabricated nanomesh structures with different polydimethylsiloxane (PDMS)/hexane weight ratios (1/40 and 1/80) to verify the optimized condition for the nanomesh-based strain sensor. The 1/40 ratio strain sensor had the highest GF of 46.3, enabling it to map facial movements during speech onto the cheek skin surface [Figure 3J]. Figure 3K presents strain distribution mapping images of the nanomesh devices compared to a PDMS thin-film device during the speech of "a". The nanomesh-based strain sensor in this work exhibited advantages of being lightweight, having a large detectable strain range, and being gas-permeable.

Transistor-based mechanical sensors

Organic material-based wearable mechanical sensors, despite their advantages of being ultrathin, lightweight, and having a simple fabrication process, still suffer from low electronic mobility, heat/humidity stability, and robustness in the air[42]. To address these challenges, a promising approach involves applying inorganic material to transistor-based sensors through microfabrication processes. In particular, inorganic thin-film transistors (TFTs) have received much attention due to their cost-effectiveness, simplicity, and rapid response times[43].

Figure 4 explains the technical development of transistor-based mechanical sensors to satisfy the mechanical and electrical properties suitable for an e-skin system. Figure 4A presents the differences between the conventional structures of metal-oxide-semiconductor field effect transistors (MOSFETs) and TFTs[44]. In terms of operation mechanism, both devices rely on the field effect in inorganic semiconductor materials. While MOSFETs offer high electrical performance due to the single crystalline material, the device must be fabricated on a limited rigid wafer. However, TFTs can be realized on an insulating substrate at relatively low temperatures, which limits the active material phase to polycrystalline or amorphous semiconductors. Figure 4B shows the typical output curve of an n-type TFT, focusing on mobility (μ) and the on/off ratio. The mobility of the TFT is the most important factor for determining the carrier transport efficiency of the semiconductor material, directly affecting the maximum drain current (I_D). The on/off ratio is simply defined as the ratio of the maximum to the minimum I_D, which should be enhanced at a constant voltage to increase the sensitivity of TFT-based sensors.

Nanomaterials have been spotlighted for application to TFT electrodes to enhance electrical conductivity, robustness, and transparency, making them suitable for next-generation displays[45]. As demonstrated in Figure 4C, Kim *et al.* reported a transparent and flexible nanoline-based field effect transistor (NL-FET) array of 254 pixels-per-inch (PPI) with high transparency (~90%), flexibility (stable at a 2.5 mm bending radius), uniformity (~90%), and high electrical performances (μ of 0.52 $cm^2/V{\cdot}s$, on/off ratio of 7.0×10^6)[46]. Figure 4D and E provides the sharp and stable switching operation of the flexible NL-FET array, maintaining its voltage gain characteristics for a complementary inverter circuit in both pristine and bent states (bending curvature radius of 2.5 mm).

To map mechanical pressure or stress changes over a large area, the common method is to create an active-matrix array and integrate TFTs into each pixel of the array. Figure 4F shows how each unit device demonstrates variations in current (I_{ON}) between contacted and non-contacted pixels, exhibiting the capabilities of transistor arrays in mapping pressure. Nela *et al.* realized a carbon nanotube (CNT)-based TFT array on a flexible polyimide (PI) substrate, characterized by rapid response time and superior sensitivity[47]. This 4-inch CNT TFT array operated at 3 V with a pressure response time under 30 ms, surpassing the responsiveness of human skin. Moreover, the flexible CNT TFTs exhibited exceptional flexibility and robustness, maintaining their device structure and electrical properties at a bending curvature radius of 5 mm.

The TFT array is utilized as a read-out device for operating multifunctional network systems with various sensors. As illustrated in Figure 4G, Someya *et al.* developed an organic transistor-integrated pressure and thermal sensor array[48]. The designed net-shaped structure with PI and poly(ethylenenaphthalate) (PEN) substrates demonstrated stable operation under uniaxial extension of 25%, adaptable for attachment to the human skin surface. Figure 4H and I shows the pressure and thermal sensor mapping images with the 12×12 device array that simultaneously measured the distribution of pressure and temperature. However, these organic-inorganic hybrid material-based devices still confront low electrical properties such as low output current due to charge transport efficiency, material stability and interface quality between organic-inorganic materials, directly affecting sensitivity[49].

Although previous works have been actively conducted to develop transparent electrodes, transferring complete transparent TFTs to target substrates remains challenging for wearable electronic systems. Direct fabrication of the TFT on a flexible substrate is considered an unresolved limitation due to the essential high-temperature annealing process. The laser lift-off (LLO) technique has arisen as a novel transfer method for flexible inorganic TFTs. Lee *et al.* reported transparent and skin-like oxide TFT array through

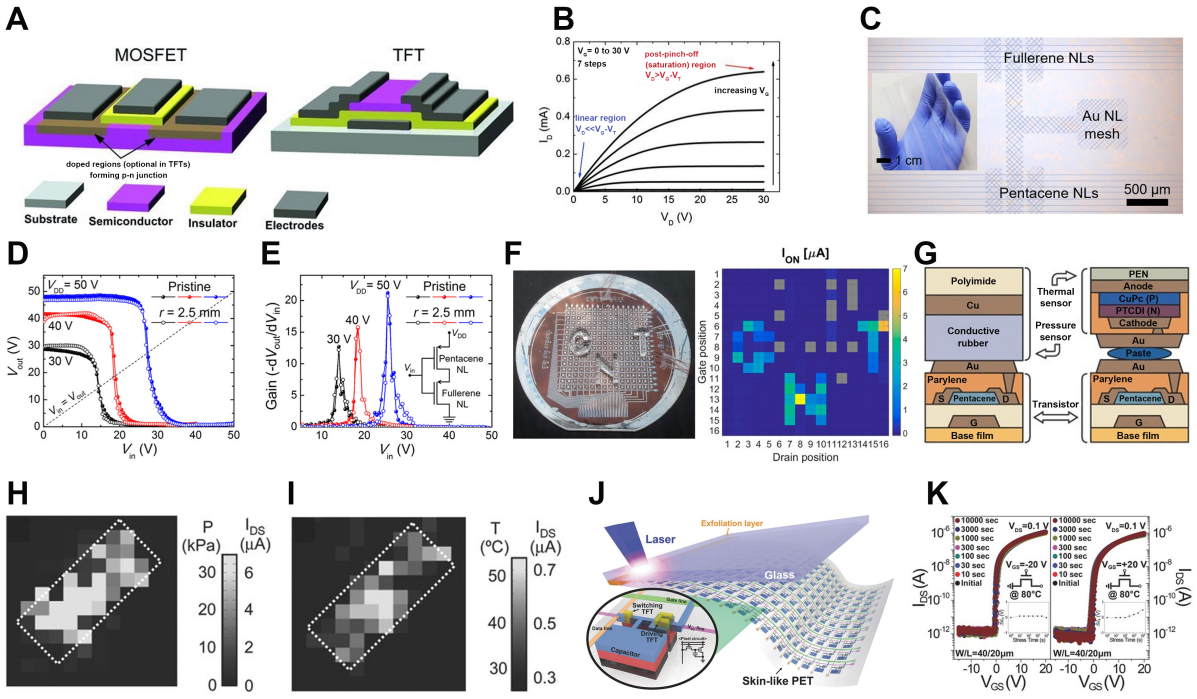

Figure 4. TFT array fabrication process with organic/inorganic materials. (A) Comparison between the typical structures of a MOSFET and a TFT; (B) Output curves of an n-type oxide TFT. Reproduced with permission from ref[44]. Copyright 2012, John Wiley and Sons; (C) Photograph (left) and optical microscopic images (right) of transparent and flexible NL-FET arrays; (D) The switching operation and (E) voltage gain characteristics of the NL-FET array under pristine and bending (r = 2.5 mm) conditions. Reproduced with permission from ref[46]. Copyright 2020, American Chemical Society; (F) Photograph and pressure mapping image using CNT-based TFT array. Reproduced with permission from ref[47]. Copyright 2018, American Chemical Society; (G) Cross-sectional illustrations of the pressure (left) and thermal (right) sensor cells using organic transistors; (H) Pressure and (I) temperature mapping images using an organic transistor-based sensor array. Reproduced with permission from ref[48]. Copyright 2015, PNAS; (J) Schematic illustration of a transparent oxide TFT array fabricated by the LLO process; (K) The stable operation of skin-like oxide TFTs under negative bias temperature stress (left) and positive bias temperature stress (right). Reproduced with permission from ref[50]. Copyright 2016, John Wiley and Sons. MOSFET: Metal-oxide-semiconductor field effect transistor; TFT: thin-film transistor; NL-FET: nanoline-based field effect transistor; CNT: carbon nanotube; LLO: laser lift-off.

the LLO method [Figure 4J][50]. When the exfoliation layer on the transparent rigid substrate is exposed to a high-energy laser pulse, the melted layer instantly forms nanostructures, reducing the adhesion force between the device layer and the substrate. By attaching the delaminated devices onto an ultrathin PET substrate, the flexible and transparent oxide TFTs were achieved, demonstrating outstanding characteristics with mobility as high as 38.5 $cm^2 \cdot V^{-1} \cdot s^{-1}$, an on/off ratio of ~ 8×10^7, a threshold voltage of -0.3 V, and optical transmittance of 83% in the visible light region. To confirm the usability of the skin-like oxide TFTs for practical transparent displays, several stability tests, including negative (NBTS) and positive bias temperature stress (PBTS) tests, have been conducted to perform excellent stability under direct illumination [Figure 4K].

Optoelectronics-based sensors

Optoelectronic devices, including light-emitting diodes (LEDs), laser, optic fiber, and PDs, have been spotlighted as a rising technology for biosensors and visualizing devices of bio-signals owing to their tunability, precise detection capabilities, and superior power efficiency[51]. Figure 5 presents state-of-the-art studies on flexible LED fabrication processes for application in e-skin systems. Figure 5A displays a flexible organic LED (OLED) on a 6 μm-thick flexible substrate for a phototherapeutic wound dressing patch, emitting 5 mW/cm^2 (670 nm) radiation in air conditions[52]. In addition, despite the instability of the organic

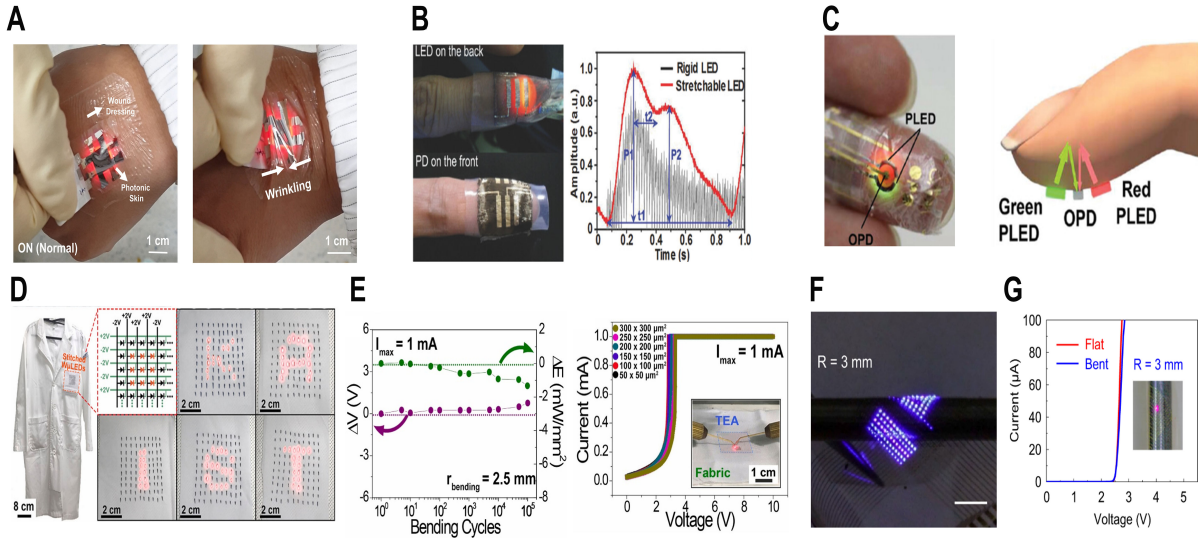

Figure 5. Flexible optoelectronics for soft electronics. (A) Photographs of an OLED photonic skin under skin-attached (left) and wrinkled state (right). Reproduced with permission from ref[52]. Copyright 2020, John Wiley and Sons; (B) Optical images of a wearable photoplethysmograph sensor with QD-LED/PD (left) and real-time PPG signal graph measured by QD-stretchable LED and -conventional LED (right). Reproduced with permission from ref[53]. Copyright 2017, American Chemical Society; (C) Photographs of a flexible PPG sensor based on PLED and OPD. Reproduced with permission from ref[54]. Copyright 2016, AAAS; (D) Photograph of a wireless WμLED, showing various alphabets; (E) Forward voltage/irradiance changes of the WμLED during 100,000 bending operations (r = 2.5 mm) (left), and I-V curves of the WμLED with various device sizes (right). Reproduced with permission from ref[56]. Copyright 2019, Elsevier; (F) Photograph of an RGB micro-LED display, attached onto a glass rod (r = 3 mm); (G) Current-voltage curve of the μLED when bent with r = 3 mm. Reproduced with permission from ref[57]. Copyright 2022, Springer Nature. OLED: Organic light-emitting diode; QD: quantum dot; LED: light-emitting diode; PD: photodetector; PPG: photoplethysmography; PLED: polymer light-emitting diode; OPD: organic photodetector; WμLED: wearable micro-scale light-emitting diode; μLED: micro-scale light-emitting diode.

material in water, the OLED demonstrated excellent reliability under a mechanical stress of 1,000 bending cycles (bending curvature radius of 1 mm) and humid conditions for an hour due to the superior passivating effect of a SiO_2-based polymer.

Recently, with the development of integrated LED/PD systems, several studies have been actively conducted to develop them as wearable PPG systems, showing high sensitivity for monitoring heart rate and SpO_2. As shown in Figure 5B, Kim *et al.* developed fully stretchable and foldable PPG sensors constructed with colloidal quantum dot LEDs (QLEDs), accomplishing a photocurrent/dark current ratio of 1.3×10^4 at 0 V and a brightness of 1,000 $cd \cdot m^{-2}$[53]. The QLEDs were transfer-printed onto pre-strained elastomers with a uniformly curved structure, allowing easy deformation without device breakdown under tensile/compressive strain. The developed stretchable QLEDs were stretched up to 70% strain without performance degradation and folded under a 35 μm bending radius with high brightness and luminous efficiency, implying that these thin QLEDs can be attached to curved surfaces or stretchable elastic substrates. Furthermore, according to the PPG recording tests, the developed stretchable QLEDs measured accurate PPG signals compared to the conventional rigid LEDs.

Yokota *et al.* reported an ultra-flexible PPG sensor based on polymer LEDs (PLEDs) and organic PDs (OPDs), demonstrating multifunctionality of simultaneous bio-signal sensing and displaying on the human skin surface [Figure 5C][54]. The passivation layer, which provides air and water resistance, was mainly investigated to extend the lifetime of the organic material-based optoelectronic devices. Particularly, the water vapor transmission rate (WVTR) was reduced to 10^{-5} g/m^2 per day by multi-stacking SiON and organic layers on a thick plastic substrate (125 μm). The developed 3 μm-thick PPG sensor maintained its performance even under a bending radius of 100 μm and measured the PPG signal on the fingertip surface.

Despite novel demonstrations, PLEDs and OLEDs have faced challenges, including low efficiency, short lifetimes, and instability in heat/humidity conditions[55]. Micro LEDs (μLEDs) offer significant advantages, such as high luminous efficacy, long lifespan, and robust endurance, under high temperatures and humid conditions. Lee *et al.* demonstrated a wirelessly powered wearable μLED (WμLED) array with high stability, enabled by transferring it onto a fabric coat [Figure 5D][56]. The 30 × 30 WμLED array was operated by receiving radio frequency (RF) electrical power, transmitted from a power supply to the wearable antenna. Figure 5E represents that the WμLED array had significant mechanical durability without device breakdown in the fatigue test with 100,000 bending motions with a 2.5 mm bending radius. The forward voltage (V_f) and irradiance (E) of the device increased by 0.76 V and decreased by only 1.33mW·mm^{-2}, respectively. In addition, the WμLED showed extreme stability even when exposed to high temperature/humidity (85 °C/85% relative humidity) detergent solutions and artificial sunlight. These results pave the road for fully functional outdoor environments with stable optoelectrical component-based sensors. Regarding the μLED size, the WμLED had negligible degradation in electrical properties [Figure 5E].

For achieving wireless sensing systems, light-based communication, including light fidelity (Li-Fi), was realized by flexible μLEDs with high bandwidth and high transmission rates. In Figure 5F, Hu *et al.* provided gallium nitride (GaN)-based μLEDs enhanced in light efficiency by adding quantum dots (QDs) and TiO_2 nanoparticles[57]. Figure 5G is the I-V curve of the flexible μLEDs with a bending radius of 3 mm, indicating a slight change in V_f regardless of the flatness of the device. The QD-coated μLED panel demonstrated a high data transmission rate of 1.9 Gbps, which also fully operated on a flexible substrate. According to these results, flexible μLEDs among diverse optoelectronic devices are suitable for various wearable sensing applications due to their superior stability, high electrical performance, and application expandability.

Human-device interfaces

Although numerous wearable systems with various optical or electrical devices have been developed, they have all shown integration with bulky conventional chips onto a wearable substrate[58]. In this case, the device delamination from the attached body occurs from the body movement-induced mechanical stresses, caused by the Young's modulus difference between the bulk chip and the wearable substrate[59]. Furthermore, when conventional flexible devices are utilized for long-term wearable sensing applications, they can lead to critical dermal problems such as skin irritation, itchiness, and inflammation due to the accumulation of skin by-products (e.g., dead cells, sebum, and sweat)[60]. In Figure 6, we introduce various human-sensing device interfaces designed to minimize skin-related issues. Kim *et al.* developed a multifunctional, chip-less, and wireless e-skin system based on a surface acoustic wave (SAW) sensor with a freestanding single-crystalline piezoelectric thin film of GaN[61]. Figure 6A compares the flexibility of the demonstrated SAW e-skin system with conventional chip-based ones. Since the SAW e-skin utilized the nanoscale GaN thin-film with an ultrathin elastomer, the device showed excellent stretchability and suitability for skin-adhesive e-skin applications with living organisms. Figure 6B presents wireless pulse measurements using the SAW e-skin strain sensors on the human wrist, highlighting their high strain sensitivity and extremely low minimum detectable strain of 0.048%. The wearable SAW sensor could monitor not only skin-applied strain but also Na^+ ions in perspired sweat by coating the device with ion-selective membranes [Figure 6C]. The membrane-penetrated Na^+ ions attached to the SAW sensor surface changed the resonant frequency of the acoustic wave. Therefore, the SAW device compares the changed frequency value, quantifying the Na^+ concentration which is a biomarker for organ failures and diseases related to psychological conditions [Figure 6D].

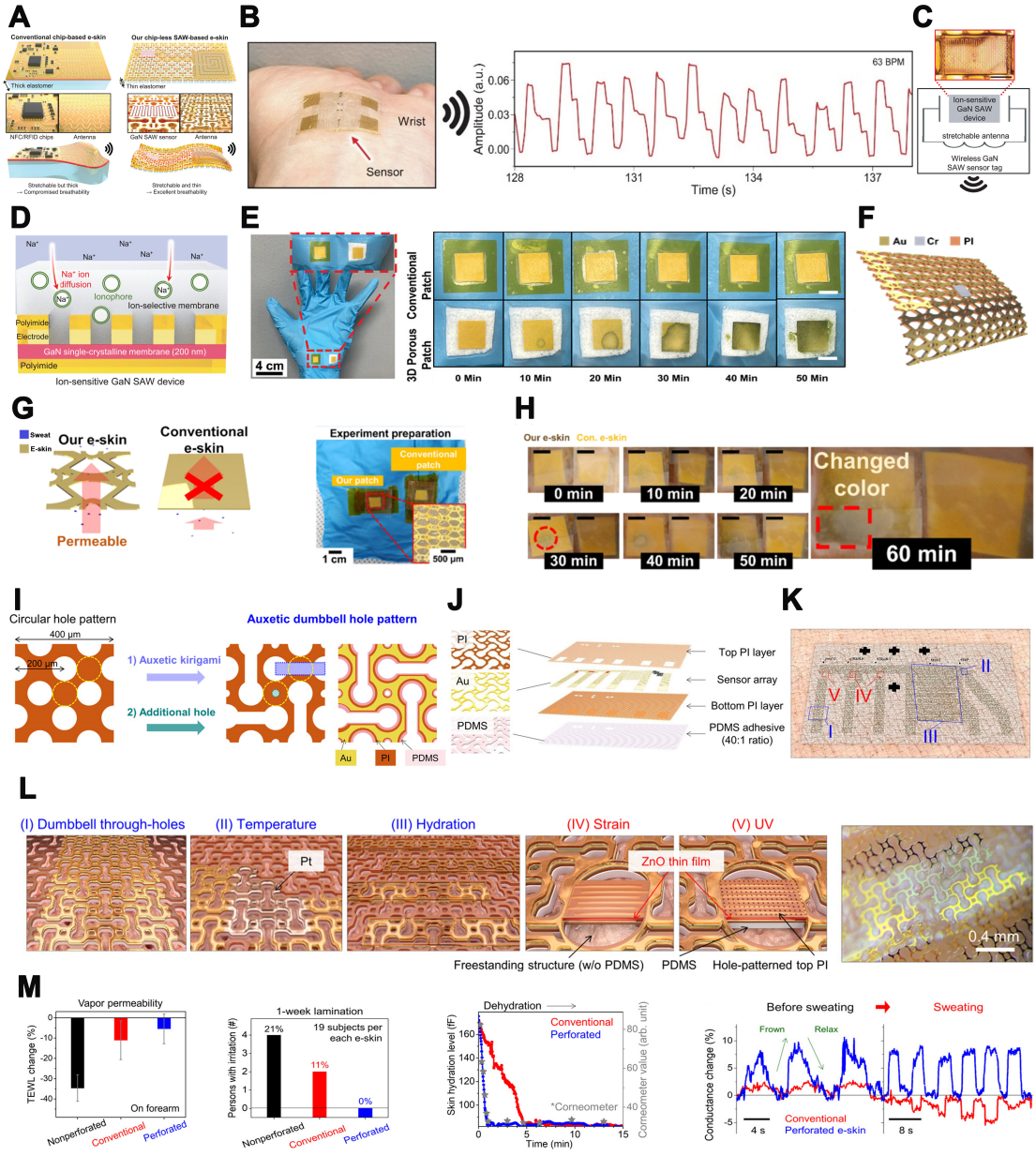

Figure 6. Perforated human-device interfaces for e-skin system. (A) Wireless e-skin based on conventional IC chips (left) and the SAW sensor-integrated wireless e-skin (right) fabricated with GaN freestanding membranes; (B) Photograph of the SAW e-skin with a strain sensor attached onto the human wrist (left) and a strain measurement graph (right); (C and D) Optical microscopic image and schematic illustration of a GaN SAW device-based wireless ion sensor. Reproduced with permission from ref[61]. Copyright 2022, AAAS; (E) Comparison of by-product removal effects in conventional and wearable patches. Reproduced with permission from ref[62]. Copyright 2023, John Wiley and Sons; (F and G) Wearable e-skin with an eye pattern for enhancing the sweat removal property; (H) Sweat removal monitoring by eye-patterned e-skin and conventional one. Reproduced with permission from ref[63]. Copyright 2023, Springer Nature; (I) Schematic illustration of the auxetic dumbbell hole pattern design for perforated e-skins; (J) 3D image of the sandwich-type e-skin fabricated with a PDMS-based adhesive layer, PI substrate layer, Au electrode, sensor semiconductor layer, and upper PI top layer; (K and L) Schematic illustrations of (I) auxetic dumbbell-patterned patch, (II) resistance-type thermometer, (III) Au-based capacitive hydration sensor, and ZnO thin-film-based (IV) strain and (V) UV sensor; (M) TEWL change after various e-skin lamination. Comparison of skin suitability of e-skin for one week. Strain sensor characteristics of the perforated e-skins and the conventional one according to skin dehydration and sweating. Reproduced with permission from ref[64]. Copyright 2021, AAAS. IC: Integrated circuit; SAW: surface acoustic wave; 3D: three-dimensional; PDMS: polydimethylsiloxane; PI: polyimide; UV: ultraviolet; TEWL: transepidermal water loss.

Recently, wearable substrates with perforated patterns have been actively investigated to prevent dermal issues by mechanically removing skin by-products over a long-term period. Kim *et al.* demonstrated a wearable and biocompatible 3D porous patch combined with InGaN/GaN-based micro-PDs (μPD) as an ultraviolet (UV) monitoring sensor[62]. The porous PDMS patch was fabricated by compressing sugar microparticles (diameter of 420~480 μm), filling them with PDMS, and removing the sugar-based mold. To verify the by-product removal property of the developed porous patch, sweat permeability tests between the 3D porous skin and the conventional one were carried out on the perspiring hand, showing rapid color changes of litmus paper within 60 minutes [Figure 6E]. Kim *et al.* suggested a mechanically stable e-skin to improve mechanical properties and sweat permeability[62]. Figure 6F displays a newly designed e-skin with porous eye patterns, incorporating a resistive-type body temperature sensor. The mechanical property of the eye pattern was analyzed with finite element analysis (FEA) simulation compared to that of other patterns, presenting lower maximum stress than the auxetic kirigami pattern, about 48.7%. Unlike the conventional e-skin, the continuous sweat removal to the outside was fulfilled by numerous holes inside the eye-pattern patch [Figure 6G]. According to the results of sweat removal tests, there was no visual change in a conventional flexible patch, but in the perforated e-skin, a large area of litmus paper (45.04 %) showed a color shift due to sweat absorption [Figure 6H]. Finally, thanks to the novel porous eye-pattern substrate, temperature sensing of the developed device was stably conducted, showing a similar measuring trend to a conventional infrared (IR) thermometer during intense exercise[63].

Yeon *et al.* engineered a sweat pore-inspired porous e-skin capable of effectively preventing sweat accumulation, thereby allowing the integrated inorganic sensors to accurately gather physical health information without malfunction[64]. Figure 6I shows the design rule of auxetic dumbbell patterns for applying conventional complementary metal-oxide-semiconductor (CMOS) fabrication processes to the perforated e-skin. The size and distribution of the holes in the dumbbell patterns were constructed to those of real human sweat pores, enabling mechanical properties similar to those of human skin. The e-skin structure was configured with a PDMS-based dry adhesive layer at the bottom, a PI substrate layer, an Au electrode, a semiconductor layer for the sensor, and a sandwich-like structure as the top PI [Figure 6J]. Furthermore, the electrode and sensor were completely embedded in PI, unaffected by electrical shorts or external moisture. Figure 6K and L explains the sensor parts in detail: (I) auxetic dumbbell-patterned patch; (II) resistance-type thermometer; (III) Au-based capacitive hydration sensor; and ZnO thin-film-based (IV) strain and (V) UV sensor. The ZnO strain sensors were realized with a freestanding structure to reduce strain damping by the PDMS layer, while the ZnO UV sensor was made with the hole-patterned top PI layer to be exposed to external UV radiation. The biocompatibility and sweat-removing ability of the developed e-skin were analyzed by transepidermal water loss (TEWL) and a 1-week device lamination test, indicating that the developed device has excellent retaining capability of the normal skin condition without any allergic reaction. In addition, the skin-attached e-skin with dumbbell patterns exhibited superior monitoring ability of external humidity and strain in a skin perspiring condition. These results suggest that the perforated e-skin with multifunctional sensors is reliable for long-term bio-signal monitoring compared to the conventional wearable patches.

IMPORTANT FEATURES APPLICABLE IN E-SKIN SYSTEMS

In e-skin systems, research has been focused not only on enhancing the sensitivity and durability of sensing devices but also on advancing the functionality of the sensor systems (e.g., external energy source for device operation and disposability for reducing electrical waste). Similar to other electronic devices, e-skin systems require an electrical energy supply to operate the sensing device. Additionally, the potential increase in the e-skin systems leads to environmental problems due to electronic wastes after use. In this chapter, we introduce features that, while not essential, apply to e-skin systems and can improve their expandability in various fields.

Electrical power sources

The ultimate objective of innovative wearable systems is to emulate real human skin, achieving imperceptibility and high comfort levels. However, the electrical wiring between the device and the external power supply is still regarded as a significant restriction for user movements[65]. To resolve this issue, several types of energy harvesters have been reported to attain self-powered electronic systems without any external power sources such as solar cells, thermoelectric power generators, and piezoelectric nanogenerators (NGs)[66].

In particular, triboelectric NGs (TENGs) have been spotlighted as a novel energy-harvesting technology due to their simple device structure, easy/fast fabrication processes, inexpensive materials, and high-power generation[67]. Figure 7A shows four fundamental TENG working modes: contact-separation, contact-sliding, single-electrode, and freestanding triboelectric layer modes[68]. The TENG, consisting of two types of materials, generates electrical power through the charge redistribution, temporarily or continuously creating a potential difference through contact and subsequent separation (contact-separation mode) or sliding motion (contact-sliding mode), respectively. Conversely, the TENG with single triboelectric material makes a potential difference with a grounded or oppositely charged object (single-electrode mode). In the freestanding triboelectric layer mode, the device generates electricity by utilizing a generated electric potential difference across the device with deformation. The TENG working mechanism combines contact electrification and electrostatic induction. The polarized triboelectric charges contribute to the voltage $V_{OC}(x)$, which depends on distance x. The transferred charges Q will also influence the electric potential difference. If the device has no triboelectric charges, it acts as a typical capacitor which is affected by capacitance and charges between the two electrodes, denoted by $-Q/C(x)$. Thus, the total voltage difference V is determined by:

$$V = -\frac{Q}{C(x)} + V_{OC}(x) \tag{3}$$

which is the fundamental relationship among Q_{SC}, C, and V_{OC}[69].

Under the short circuit (SC) conditions, the transferred charges (Q_{SC}) are completely generated from polarized triboelectric charges where V is 0:

$$Q_{SC}(x) = C(x)V_{OC}(x) \tag{4}$$

Gai *et al.* reported a self-powered wearable sweat analysis system (SWSAS) by hybridizing TENG and an electromagnetic generator (EMG), which harvested electrical energy from human motion through two hybrid NG modules (HNGMs)[70]. The SWSAS selectively monitored biomarkers of Na^+ and K^+ in human sweat, wirelessly transmitting the sensing data via a Bluetooth module. By applying external force, the polytetrafluoroethylene (PTFE) film at the TENG center contacts and makes sliding friction with both sides of the nylon films, resulting in negative charge accumulation due to the difference in triboelectric polarity. On the other hand, the surface of the nylon film accumulates an equivalent number of positive charges [Figure 7B (i-iii)]. The repetitive, vertical movement of the PTFE film generates an electron flow due to the potential difference, resulting in a continuous alternating current (AC) output [Figure 7B (iv)]. Figure 7C shows the working principle of the EMG. Initially, the magnet is fixed to the upper coil, showing no current

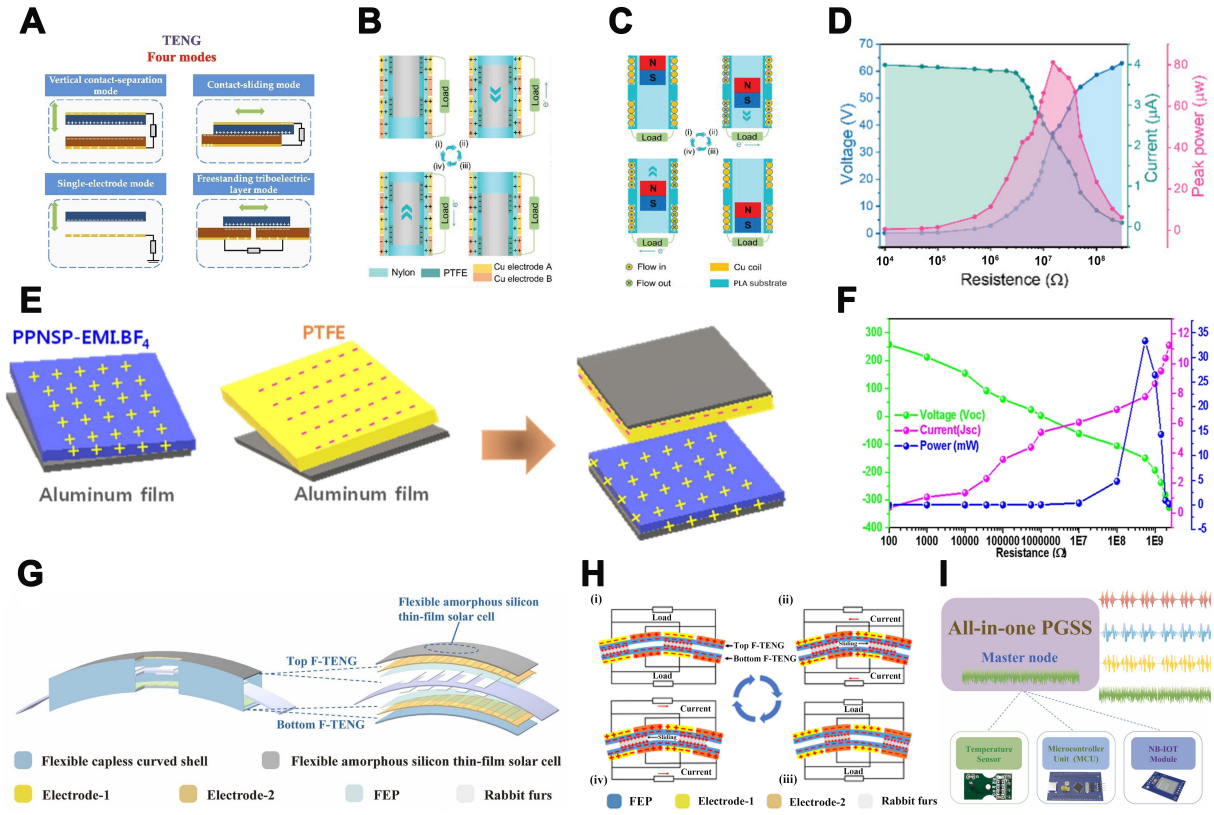

Figure 7. TENG module for e-skin systems. (A) Four TENG modes: vertical contact-separation mode, lateral sliding mode, single-electrode mode, freestanding triboelectric-layer mode. Reproduced with permission from ref[68]. Copyright 2021, Elsevier; Schematic illustration of (B) the TENG and (C) the EMG operating mechanism; (D) V_{oc}, and I_{sc} graph of the HNGM integrated with TENG and EMG. Reproduced with permission from ref[70]. Copyright 2022, John Wiley and Sons; (E) Schematic illustration of the polymeric membrane-based energy harvester; (F) Graph of output power against external load resistance at 5 Hz. Reproduced with permission from ref[71]. Copyright 2022, Springer Nature; (G) Schematic illustration of A-PGSS with TENG and f-SC; (H) Operation principle of the A-PGSS; (I) Scheme of the all-in-one PGSS with low-power conventional LP-SCC, LP-MCU, and BLE. Reproduced with permission from ref[72]. Copyright 2023, Elsevier. TENG: Triboelectric nanogenerator; EMG: electromagnetic generator; HNGM: hybrid nanogenerator module; A-PGSS: all-in-one power-generating and sensing system; PGSS: power-generating and sensing system; f-SC: flexible solar cell; LP-SCC: low-power conventional signal conditioning circuit; LP-MCU: low-power microcontroller unit; BLE: Bluetooth low energy.

in the coil. After the downward movement of the magnet, the change in magnetic flux across the coil generates an electrical current to equalize the charge of the upper coil with that of the lower one. As the magnet moves upward, the magnetic flux crossing the coils is induced in the opposite direction, resulting in a reverse current. Figure 7D exhibits the output power for charging a 330 μF capacitor by TENG, EMG, and HNGM. The HNGM, consisting of TENG and EMG, solved the shortages of each device by integrating/engineering the high output voltage (V_{oc}) of the TENG and the superior output current of the EMG.

To apply the power source to e-skins, the TENG requests properties of flexibility, stretchability, and durability corresponding with human skin. As shown in Figure 7E, a polymeric membrane-based energy harvester was reported to realize highly flexible e-skin with TENG, fabricated by PEDOT:poly(styrenesulfonic acid) (PSSa)-naphthalene sulfonated PI [(PPNSP)-EMI.BF_4][71]. The PPNSP e-skin with a porous network continuously transported ions through nano-channels, producing strong molecular attracting-repulsing interactions with intrinsic ions. In addition, V_{oc} (109 V) and high output current (I_{scs}) (2.35 μA) were induced by doping EMI.BF_4 ionic liquid (IL) into the PPNSP skin due to active inter-exchange of ions. In the TENG application, the PPNSP-EMI.BF_4 e-skin and the PTFE film with aluminum

electrodes repeatedly contacted and separated to generate a maximum output power of 33.2 mW [Figure 7F].

With the increasing requirement of wearable energy harvesters for daily use, Liu *et al.* demonstrated an all-in-one power-generating and sensing system (A-PGSS) based on TENG and flexible solar cell (f-SC)[72]. Figure 7G shows a structural design of the A-PGSS with two rabbit fur-based TENGs and one amorphous Si-based SC. When the rabbit fur with good tribo-positivity and low friction resistance moves by external force, electrons flow to the opposite electrode through an external circuit, maintaining electrostatic balance between the two electrodes and generating a brief current [Figure 7H (i) and (ii)]. Negative charges accumulate on the fluorinated ethylene propylene (FEP) membrane surface, while the rabbit fur surface accumulates an equal number of positive charges. When the rabbit fur slider moves back, electrostatic equilibrium is disrupted in the fourth stage, causing positive charges on electrode-2 to flow in the opposite direction, towards electrode-1, resulting in a reverse transient current in the external circuit [Figure 7H (iii) and (iv)]. The fabricated A-PGSS produced a maximum power density of 0.072 W/m^2 (load resistance: 3 MΩ) at a 2.5 Hz contact frequency. Finally, the authors demonstrated the usability of A-PGSS with low-power conventional signal conditioning circuit (LP-SCC), low-power microcontroller unit (LP-MCU) and Bluetooth low energy (BLE) under daily life conditions such as daytime, nighttime and emergencies [Figure 7I].

Biodegradable sensors

E-skins are expected to be mainly used as disposable products. However, considering the environmental destruction caused by electronic waste, which is a severe issue due to the exponential development of electronic devices, the development of biodegradability is an essential factor for e-skins in healthcare applications[73]. Figure 8A shows biodegradable materials for substrates, electrodes, semiconductors, dielectrics, encapsulants, and adhesives according to their applications in implantable and non-invasive sensors[74]. The biodegradable properties of these materials are suited to monitor temporary phenomena such as wound healing, aftereffects, and side effects. Veeralingam *et al.* reported a $NiSe_2$-grown cellulose paper with silver paste for a low-cost and disposable sensing platform that can be applied to pH meters, breath analysis, and strain sensors[75]. The cellulose paper-based flexible substrate was dipped in a seed solution with selenium powder, sodium borohydride, and $NiCl_2$ in deionized (DI) water for about one hour. The seed-coated cellulose paper was transferred to a Teflon autoclave for a hydrothermal reaction at 200 °C for 20 h. Thereafter, the $NiSe_2$/Cellulose paper was dried at 70 °C and integrated with an Ag electrode to realize a breath sensor [Figure 8B]. Figure 8C presents the breath sensing results for one minute. The current of the sensor increased during exhalation, whereas the device current decreased during inhalation.

Wang *et al.* developed a highly strain-sensitive, fast-responding, stable, and biodegradable e-skin using silk fibroin (SF) as a structural basis, combined with a hydrogel and a flexible conductive film electrode[76]. The biodegradable e-skin was fabricated with a SF/polyvinyl alcohol (PVA) hybrid film and a SF-based hydrogel. The SF/PVA film was manufactured with SF/PVA mixed solution using the solution casting method, and the hydrogel was obtained with horseradish peroxidase (HRP)-blended. Figure 8D illustrates the fabrication process of the SF-based pressure sensor using SF/PVA hybrid film and SF hydrogel with an enzymatic crosslinking method. The hierarchical structure of SF enabled the design of elastic hydrogels with resilience and flexible films with a porous structure with high deformability. The fabricated SF sensor could accurately sense a wide surface area of pressure due to its variable capacitance depending on pressure. Figure 8E shows excellent properties of the biocompatible and biodegradable sensor such as a high strain sensitivity of 4.78. The SF sensor also demonstrates fast responsiveness of < 0.1 s and superior durability for 20,000 cycles of 20% stretching. Figure 8F and G presents an 8 × 8 array of SF-based sensors for mapping the pressure by gathering the capacitance change of each unit sensor. The detailed vertical and horizontal pressure data was used to generate a mapping image of the pressure distribution in 3D [Figure 8G].

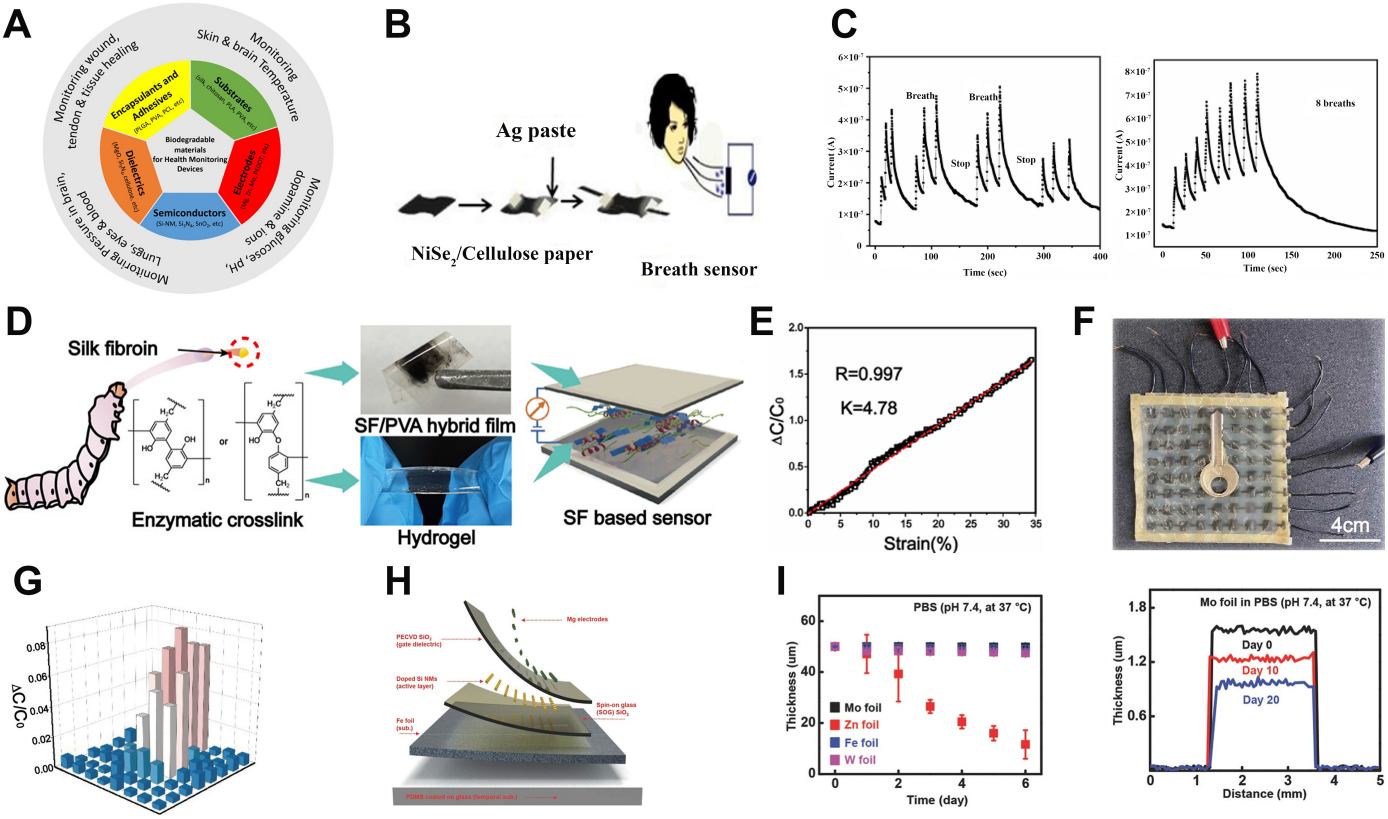

Figure 8. Biodegradable materials and sensor device for soft electronics. (A) Circular diagram of biodegradable materials for realizing a health monitoring device. Reproduced with permission from ref[74]. Copyright 2020, American Chemical Society; (B) Fabrication diagram of a $NiSe_2$/Cellulose paper-based breath sensor; (C) Breath pattern monitoring by the $NiSe_2$/Cellulose paper-based breath sensor. Reproduced with permission from ref[75]. Copyright 2019, American Chemical Society; (D) Image of a biodegradable pressure sensor, which was fabricated by SF hydrogels and SF/PVA hybrid films; (E) Electrical properties of the biodegradable SF-based pressure sensor; (F) SF-based e-skin with 64 pixels for mapping the pressure distribution; (G) Pressure distribution using the SF-based e-skin; (H) Exploded view of a transient n-channel MOSFET array on a biodegradable Fe foil. Reproduced with permission from ref[76]. Copyright 2022, American Chemical Society; (I) Measured dissolution kinetics of metal foils in pH 7.4 PBS at 37 °C (left). Line scan profiles of Mo thickness changes (right). Reproduced with permission from ref[80]. Copyright 2015, John Wiley and Sons. SF: Silk fibroin; PVA: polyvinyl alcohol; MOSFET: metal-oxide-semiconductor field effect transistor; PBS: phosphate-buffered saline.

Despite the fast advancements in the biodegradable and mechanical properties of polymer substrates, the electrode materials have faced significant issues, such as swelling, cracking, and dissolving, due to their poor stability in the external environment[77]. Therefore, several researchers have investigated biodegradable metal films (e.g., Ti and Al) with notable mechanical stability for application to biomedical devices as electrode materials[78,79]. Kang *et al.* reported the transient electronics with biodegradable metal foils (Fe, Mo, W, and Zn)[80]. Figure 8H displays an exploded view of a transient n-MOSFET array with Mg electrodes, SiO_2 gate dielectric, and Si nanomembrane active layer on a Fe foil. Figure 8I shows the dissolution kinetics of various biodegradable metal foils in phosphate-buffered saline (PBS) solution with a pH of 7.4. The changes of each film thickness in PBS were 0.02 (Mo), 0.08 (Fe), 0.15 (W), and 3.5 (Zn) μm/day, respectively. The Mo foil particularly showed a uniform thickness decrease in PBS, as shown in the right graph of Figure 8I. Because of the uniform removal of the Mo foil in the PBS solution, the fabricated MOSFET exhibited stable operation for about 5 h.

HEALTHCARE APPLICATIONS

Vital monitoring devices

Thin film-based flexible sensors have opened the possibility of vital sign monitoring of skin, organs, and body movements due to their conformal attachability to body organs[81-83]. For detecting biological problems, several research groups have demonstrated wearable sensors for analyzing various homeostatic biomarkers such as heartbeat, sweat ion concentration, tears, and saliva[84-88]. Kang *et al.* reported a low-power heterojunction phototransistor to monitor the PPG signal [Figure 9A][89]. The PPG sensor was fabricated using the poly{3-[(2,2':5',2''-terthiophen)-5-yl]-2,5-bis(2-octyldodecyl)-2,5-dihydropyrrolo[3,4-*c*]pyrrole-1,4-dione-6,5''-diyl} (DPP2ODT2-T) layer with chlorobenzene (CB) and toluene (Tol), accomplishing a stable voltage level and low power consumption (5 V) for accurate sensing under various heart rates. The superior electrical/optical properties of the sensor provide long-term and accurate sensing capabilities under different heart rate conditions in cardiovascular checks.

Invasive blood tests for analyzing ion concentrations, such as Na^+, K^+, and Cl^- or glucose, are applied in various fields (electrolyte analysis, pH tests, and diabetes), but they have significant issues such as skin trouble, wounds, and pain[90-92]. The potentiometric sensors measure the potential difference between a reference electrode and a working electrode to track the change of the ion concentrations against time. With their simplicity, diverse ion detection capabilities and rapid response times, potentiometers have been spotlighted in diverse fields, especially in ion sensing of body fluid[93,94]. Sweat analysis with potentiometric sensors has been considered as an invasive vital monitoring method; however, several obstacles remain, such as limitations of sweat collection, materials toxicity, and low multi-sensing capabilities.

Criscuolo *et al.* developed a multifunctional sweat analyzing system, integrating ion-selective membranes and cotton microfluidics for stable and continuous monitoring [Figure 9B][95]. The system consisted of four ion-selective electrodes for each ion: Na^+, Li^+ (therapeutic drug), Pb^{2+} (heavy metals exposure), and K^+ (hydration and activity). The multifunctional sweat sensors were fabricated using conventional micro-electro-mechanical systems (MEMS) processes, demonstrating stable sensing properties in water and artificial sweat, even under mechanical stress (180° bending). To prove real-time monitoring applications, the sodium and potassium levels were tracked by the wearable system, showing high Pearson correlation coefficients of about 0.97 (Na^+) and 0.81 (K^+) during physical exercise of five human volunteers. These results mean that the developed wearable sweat sensing system has the potential for the non-invasive vital sign monitoring technology.

Since various mechanical oscillations/movements (e.g., voices, heartbeats, and tremors) occur in our body, monitoring them is important to check bio-stability. To distinguish small bodily oscillations, high sensitivity and signal separation properties of the devices are required. Although several researchers have reported the wearable strain sensor with high sensitivity over 1 kPa^{-1} and GF of ~10^3 under 2%~6% strain, these strain sensors have various issues including high-cost/complex manufacturing processes, and low stability under harsh environmental conditions[96-101]. Tolvanen *et al.* developed a stretchable and washable crack sensor using silver ink-patterned silicone elastomer [Ag-dragon skin with conductive fiber (Ag-DS/CF)] [Figure 9C][102]. This strain sensor was fabricated in the pre-stretching state to withstand the dynamic loading-induced strain by forming the wrinkle of Ag-ink. Depending on the intensity of the applied strain, the change of the device sensitivity was inversely proportional, providing action detectivity regardless of its size. The fabricated strain sensor exhibited a high GF of 1.2×10^5 and negligible hysteresis loss under the repeated stretching cycles. This crack-based strain sensor with the maximum pressure sensitivity of 0.82 kPa^{-1} at 0.035 kPa demonstrated the notable sensing properties under body movement and steel ruler oscillation [Figure 9D].

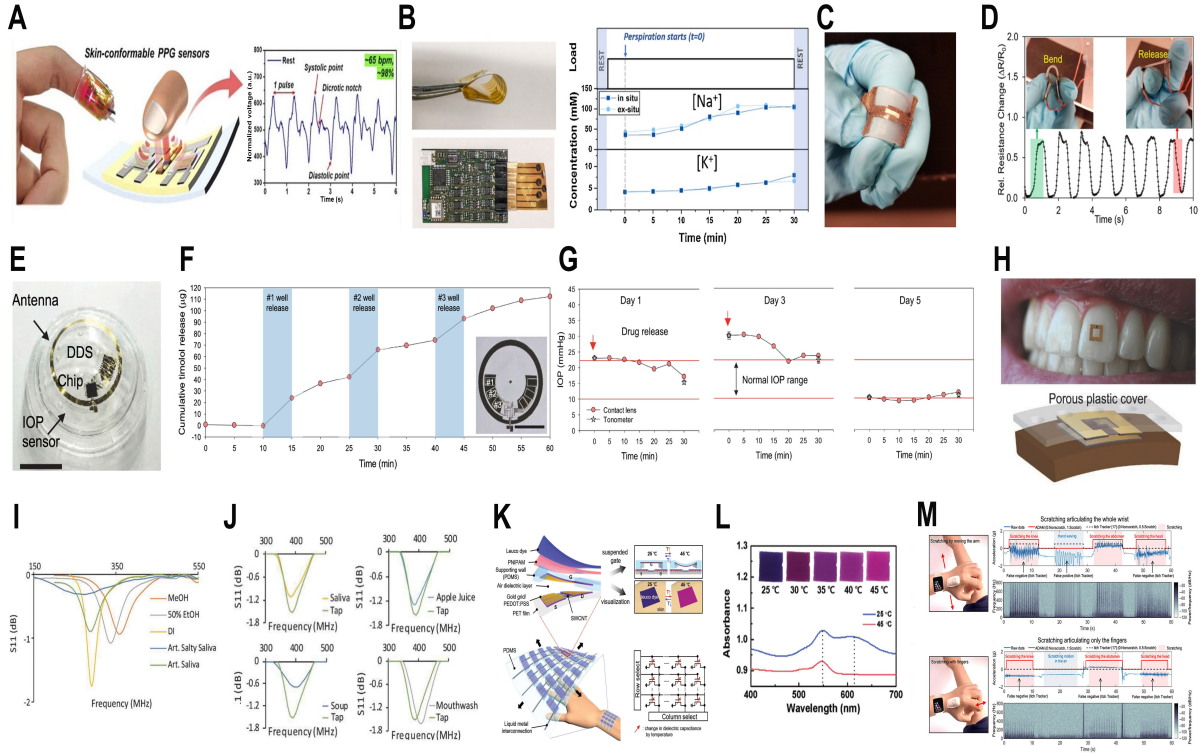

Figure 9. Healthcare monitoring wearable devices with various bio-signals. (A) Image of a skin-conformable PPG sensor and its heart rate monitoring. Reproduced with permission from ref[89]. Copyright 2021, Elsevier; (B) Sweat sensor system for monitoring ions (left) and real-time monitoring results of K^+ and Na^+ in the perspiration (right). Reproduced with permission from ref[95]. Copyright 2020, Elsevier; (C) Photograph of the Ag-DS/CF sensor under finger bending strain; (D) Resistance changes of Ag-DS/CF in bending and releasing cycles. Reproduced with permission from ref[102]. Copyright 2018, Springer Nature; (E) Optical image of theranostic smart contact lenses (scale bar, 5.5 mm); (F) I-t curve of the flexible DDS with different three drug containers. (G) IOP monitoring with timolol release from Day 1 to Day 5. Reproduced with permission from ref[108]. Copyright 2022, Springer Nature; (H) Photograph of the wireless saliva sensor; (I and J) Various solution responsivity of wireless saliva sensor. Reproduced with permission from ref[109]. Copyright 2018, John Wiley and Sons; (K) Schematic illustration of a skin-attachable, stretchable TSFET device with a suspended gate and thermochromic display; (L) Absorbance spectra of the thermochromic leuco dye film at 25 and 45 °C. Reproduced with permission from ref[111]. Copyright 2018, Elsevier; (M) Motion detecting characteristics of the ADAM device on the dorsal hand, compared to conventional devices. Reproduced with permission from ref[112]. Copyright 2022, AAAS. PPG: Photoplethysmogram; Ag-DS/CF: Ag-dragon skin with conductive fiber; DDS: drug delivery system; IOP: intraocular pressure; TSFET: temperature sensor based on field effect transistor; ADAM: advanced acousto-mechanic.

Intraocular pressure (IOP), the pressure within the eye, must be consistently monitored to prevent significant ocular diseases such as glaucoma and ocular hypertension[103-105]. Smart contact lenses with DDSs have been reported for IOP response but faced some issues such as low sensitivity, biocompatibility, and stability for long-term IOP monitoring[106,107]. As displayed in Figure 9E, Kim *et al.* developed a theranostic smart contact lens composed of a sensitive gold hollow nanowire-based IOP sensor, a flexible DDS, wireless power/communication systems, and an integrated circuit chip for controlling IOP to treat glaucoma[108]. The system achieved superior IOP sensitivity and stability with high transparency of 84% for long-term usable lens. Furthermore, the flexible DDS system had biocompatibility and high drug loading efficiency (~85%), enabling practical IOP control. Figure 9F shows the timolol releasing properties from the smart lens, which is the medicine for controlling IOP. The smart lens was inserted at the eye of a glaucoma-infected rabbit, measuring the IOP and treating high IOP state via timolol release [Figure 9G]. The developed smart lens showed the potential for expandability of wearable biomedical sensors.

Tseng *et al.* reported a wireless saliva sensor consisting of a silk film and a poly(N-isopropylacrylamide) (PNIPAM) responsive hydrogel[109]. This wearable saliva sensor was attached to tooth enamel, enabling the determination of the kind of food being eaten by monitoring changes of the resonant frequency [Figure 9H]. The PNIPAM hydrogel was responsive to a wide range of fluid properties, including alcohol content, salinity, sugars, pH, and temperature. The fabricated sensor distinguished the materials by comparing RF change under DI water, artificial saliva, 50% alcohol, methanol, and high salinity saliva [Figure 9I]. Compared to DI water, artificial saliva revealed a lower amplitude (and slightly lower resonant frequency) owing to its higher ionic strength, while alcohol caused an increase of the resonant frequency due to a lower net permittivity. Four kinds of foods were eaten by the subject, showing different resonance frequencies [Figure 9J]. The reported wearable saliva sensor opened the opportunity to provide immediate treatment to patients who have ingested hazardous food via its real-time pH sensing characteristics.

Among the five senses, visual information is the most powerful and memorable due to its high storability of ~78%[110]. Therefore, numerous researchers have paid attention to the visually vital sign info-communication device with wearable patches. Hong *et al.* demonstrated a temperature sensor based on FET (TSFET) with visual communication via leuco dye[111]. The TSFET utilized a suspended gate using PNIPAM, which changed the drain current as airgap decreased with increasing temperature, as shown in the upper right image of Figure 9K. Leuco, with an easy coating process and low cost, displayed various colors according to its structural change, resulting in the device sensitivity of 6.5%/°C in the temperature range between 25 and 45 °C. Furthermore, the thermochromic leuco dye showed a transmittance peak shift to the long wavelength under due to increased temperature [Figure 9L]. This suggested temperature sensor was an innovative approach demonstrating that the electrical signals can be replaced with visual signals.

Recently, strain sensors with high sensitivity, stability and robustness have been reported; detecting specific movements, such as finger, wrist and fine vibrations of skin, remained challenging. Chun *et al.* presented a skin-conformable wireless mechanical sensor to profile various hand and specific body movements using advanced acousto-mechanic (ADAM) sensors[112]. The ADAM sensor was placed on the dorsum of the hand and captured acousto-mechanic signals from ambient noises. Figure 9M compares the obtained scratching movements by moving the arm and fingers. The comparison was conducted with two modes of scratching: one by the arm and the other by only the fingers. The blue line represented the time series of the raw data, and the red line indicated the final binary classification results, where 0 and 1 correspond to non-scratch and scratch, respectively. To apply the ADAM system to practical applications, an algorithm-based study was performed, and the ADAM system showed an accuracy of 99.0% against visual observation. This work highlighted the potential wide-ranging applications from assessing the efficacy of drugs for conditions causing itchiness to monitoring disease severity and treatment response.

Biomedical therapeutic devices

In recent decades, many researchers have developed e-skin-based treatment methods to address the medical inconveniences such as invasive treatments and in-hospital care. Innovative e-skin technologies using opto-devices, electric fields (EFs), and microneedles have attracted attention due to their non-invasiveness, convenience, and low side effects. Figure 10 explains biomedical treatment devices integrated into the e-skin systems. Since alopecia is a common disease with a wide age range of onset, treatment methods have been developed such as minoxidil (MNX), finasteride, and surgical hair transplants, but these approaches have low efficiency and side effects[113-115]. Lee *et al.* reported a wearable photostimulator for hair growth applications through flexible red vertical μLEDs (f-VLEDs) with high output power (~30 mW/mm^2) and low V_f bias (~2.8 V)[116]. Figure 10A compares the hair growth rate of rat groups between f-VLED and MNX treatment. After 20 days of treatment, the hair length of the photostimulated mouse was 183.2 μm, approximately 76.8% longer than that of the MNX group (103.6 μm). Figure 10B compares stained tissues

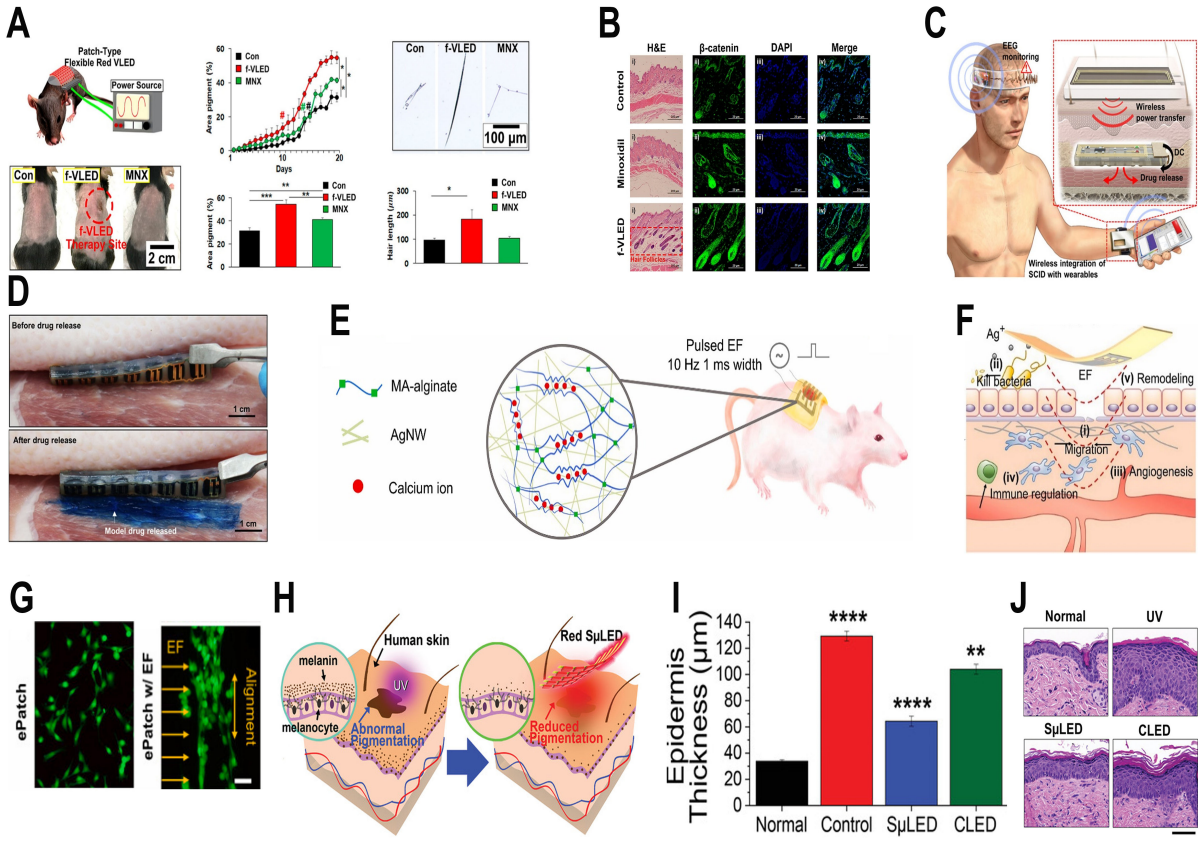

Figure 10. Medical actuators for therapeutic applications. (A) Graphical figuration of trichogenic photostimulation with monolithic red f-VLEDs and mouse dorsal skin comparison about hair-regrowth effect (left). Comparison of the hair-grown skin area, the hair-growing speed, and the grown hair length after various skin stimulations (center). $^{*}P < 0.05$, paired *t* test, $\#P < 0.05$, two way ANOVA; $^{**}P < 0.01$, $^{***}P < 0.001$, paired *t* test (center), $^{*}P < 0.05$, paired *t* test (right); (B) Immunofluorescence analysis of the stimulated mouse dorsal skin. Reproduced with permission from ref[116]. Copyright 2018, American Chemical Society; (C) Schematic illustration of an SID and a wearable EEG monitoring device with a wearable power transfer unit. The inset shows drug releasing mechanism of the SID with an activation signal from wireless power transfer; (D) Model drug releasing image of the SID which is attached onto porcine skin. Reproduced with permission from ref[117]. Copyright 2021, AAAS; (E) Schematic image of an AgNW-MAA ink-based ePatch for realizing wound healing through pulsed EF; (F) Biological activities of the healing process with the ePatch attachment; (G) Stained live cell distribution with the ePatch (left) and cell grown with EF groups after applying EF for 24 h (right). Cells are aligned in lines indicated by the yellow arrows. Reproduced with permission from ref[118]. Copyright 2022, Elsevier; (H) Schematic image of photostimulation for melanogenesis inhibition via the SμLED patch; (I) Diagram of photodamaged skin thickness, each treated with control, SμLED, and CLED. $^{**}P = 0.01$, and $^{****}P = 0.0001$; (J) H&E-stained images of mouse skin after photostimulations in 20 days. Reproduced with permission from ref[119]. Copyright 2022, John Wiley and Sons. f-VLEDs: Flexible red vertical micro-scale light-emitting diodes; SID: soft implantable drug delivery device; EEG: electroencephalography; AgNW-MAA: silver nanowire-methacrylated alginate; EF: electric field; SμLED: surface-lighting micro-light-emitting diode; H&E: hematoxylin and eosin.

and hair follicles under each treatment condition to confirm the correlation between red light and hair follicle cell proliferation. Mice in the experimental group demonstrated local hair regrowth in light-irradiated regions, while control groups exhibited negligible changes.

Recently, accurate drug dosing methods have been developed using the implantable DDSs with a wearable structure for reducing the drug abuse risk. Figure 10C shows the RF-based wireless DDS for monitoring and treating epileptic seizures[117]. The soft implantable drug delivery device (SID) consisted of a drug reservoir (parylene), epoxy to prevent drug leakage, and platinum pads for electrolysis electrodes. The drug delivery method followed these steps: (1) the electroencephalography (EEG) sensor detected the abnormal signal caused by an epileptic seizure; (2) the external RF sensor transmitted the electrical signal; (3) water in the

SID was decomposed via electrochemical reaction; and (4) the bubbles increased the internal pressure, inducing the SID drug release [Figure 10C]. Figure 10D exhibits the drug releasing results by utilizing the implanted SID in pig skin tissue. The EEG and epileptic seizure signals were measured by the algorithm, and the model drug (Evans blue) was successfully released through the measured signals.

Since secondary infection from existing wounds can lead to various problems such as high fever, edema, and convulsion, several ointment-type drugs have been developed. However, these drugs must be applied multiple times according to the severity of the wound. To solve this issue, a wound treatment patch based on EF stimulation has been developed by Wang *et al.*[118]. A flexible wound healing electrical patch (ePatch) applying the EF to the wound region was realized using conductive hydrogel electrodes [Figure 10E]. As shown in Figure 10F, the wound healing was assisted by cell migration and proliferation, induced by the EF. Figure 10G presents the comparative images of the fibroblast alignment with and without the EF. When the EF was not applied, the fibroblast migration and alignment were not observed. In contrast, when the EF was applied, both migration and alignment were evident.

In addition to treating diseases, phototherapeutic devices have recently gained popularity as skincare tools. However, most optical skincare devices for home-care use have been made with bulky LEDs, providing non-uniform light irradiation and beauty care effects. Lee *et al.* accomplished a surface-lighting micro-LED (SμLED)-based wearable patch for uniform melanogenesis inhibition [Figure 10H][119]. The SμLEDs with 630 nm of wavelength were adequate to prevent melanogenesis on the skin and were monolithically fabricated on a plastic substrate. Moreover, the SμLED exhibited outstanding mechanical stability under 10^5 bending cycles at a 5 mm bending radius and endured a harsh environment within 100 days under 85 °C/85% relative humidity. According to the melanogenesis inhibition tests, the SμLED-based patch efficiently reduced the melanin cells without any skin photodamage [Figure 10 (i) and (j)]. These results confirmed that wearable patches with multifunctionality by integrating various electrical components could non-invasively treat various diseases and be applied in the beauty care field.

CONCLUSION AND OUTLOOK

This review summarized the latest and most sophisticated stages of e-skins and flexible sensing/treating technology for personalized wearable biomedical healthcare. Various materials, including conductive polymers, nanomaterials, and inorganic semiconductors, have been utilized to enhance the electrical and mechanical properties of the e-skin. Flexible e-skin components with strain-pressure sensors, TFTs, optoelectrical sensors, and device substrates allowed the integration of multifunctional e-skin systems for monitoring human health vitals such as heart rate, ion concentration, IOP, and body motions. Independent and wireless electrical systems could be achieved by adopting TENGs that replace the external power supply, adding biocompatibility using biodegradable materials. Furthermore, wearable therapeutic apparatus provided precise treatment with alopecia, seizures, skin wounds, and melanogenesis inhibition. Despite advancements in e-skin technology, some challenges remain as follows: The reported sensors are unreliable in harsh conditions of high temperature, humidity, and heavy mechanical impact. While most studies have concentrated on enhancing the sensing capabilities of devices, their reliability in these conditions has yet to be confirmed. Furthermore, since the developed devices are directly attached onto the organ, the durability of the e-skin system has to be guaranteed under periodic and high strain conditions during human movement. To achieve multifunctionality, although several sensor devices need to be integrated into a single system, the high-density integration of devices generates excessive heat, leading to organ damage, device degeneration, and fluctuations in sensitivity. Because signal noise is considered as a critical and inevitable issue in every sensor system, the packaging technique with electromagnetic shielding has been actively investigated to minimize inaccurate signal analyses during long-term usage. Despite these

challenges, multifunctional wearable systems have been developed to achieve a wide range of personal health monitoring devices connected with the internet of things (IoT)[120]. The integrated sensor systems with large deformation proof, multi-module integration, multi-signal sensing, and fast response rate will comprehensively enhance the body-attachable e-skins for biomedical applications. The rapid advancements of e-skin systems are expected to revolutionize the healthcare industry and introduce new personalized medical platforms without any spatiotemporal limitations.

DECLARATIONS

Authors' contributions

Conceptualization, writing original draft: Kim KH
Revising the manuscript: Kim JH
Figure editing, investigation: Ko YJ
Project administration, supervision, review, and editing: Lee HE

Availability of data and materials

Not applicable.

Financial support and sponsorship

This work was supported by the Commercializations Promotion Agency for R&D Outcomes (COMPA) grant funded by the Korean Government (Ministry of Science and ICT,2023) and the National Research Foundation of Korea (NRF) grants funded by the Ministry of Science, ICT and Future Planning (MSIT) (RS-2023-00278906, and NRF-2022R1A4A3033320).

Conflicts of interest

All authors declared that there are no conflicts of interest.

Ethical approval and consent to participate

All experiments involving humans or animals cited in the figures within the text have been reviewed and approved by the relevant ethics committee, and for human experiments, informed consent has been obtained from the participants.

Consent for publication

Not applicable.

REFERENCES

1. Ge D, Mi Q, Gong R, et al. Mass-producible 3D hair structure-editable silk-based electronic skin for multiscenario signal monitoring and emergency alarming system. *Adv Funct Mater* 2023;33:2305328. DOI
2. Dong Y, Xu D, Yu H, Mi Q, Zou F, Yao X. Highly sensitive, scrub-resistant, robust breathable wearable silk yarn sensors via interfacial multiple covalent reactions for health management. *Nano Energy* 2023;115:108723. DOI
3. Xu D, Ouyang Z, Dong Y, et al. Robust, breathable and flexible smart textiles as multifunctional sensor and heater for personal health management. *Adv Fiber Mater* 2023;5:282-95. DOI
4. Thacker SB, Stroup DF, Sencer DJ. Epidemic assistance by the centers for disease control and prevention: role of the epidemic intelligence service, 1946-2005. *Am J Epidemiol* 2011;174:S4-15. DOI PubMed PMC
5. Ding X, Clifton D, Ji N, et al. Wearable sensing and telehealth technology with potential applications in the coronavirus pandemic. *IEEE Rev Biomed Eng* 2021;14:48-70. DOI
6. Wang Y, Zhao C, Wang J, et al. Wearable plasmonic-metasurface sensor for noninvasive and universal molecular fingerprint detection on biointerfaces. *Sci Adv* 2021;7:eabe4553. DOI PubMed PMC
7. Li Q, Zhang LN, Tao XM, Ding X. Review of flexible temperature sensing networks for wearable physiological monitoring. *Adv Healthc Mater* 2017;6:1601371. DOI PubMed

8. Dincer C, Bruch R, Costa-Rama E, et al. Disposable sensors in diagnostics, food, and environmental monitoring. *Adv Mater* 2019;31:e1806739. DOI
9. Nikolic MV, Milovanovic V, Vasiljevic ZZ, Stamenkovic Z. Semiconductor gas sensors: materials, technology, design, and application. *Sensors* 2020;20:6694. DOI PubMed PMC
10. Ren Z, Yang J, Qi D, et al. Flexible sensors based on organic-inorganic hybrid materials. *Adv Mater Technol* 2021;6:2000889. DOI
11. Prosa M, Bolognesi M, Fornasari L, et al. Nanostructured organic/hybrid materials and components in miniaturized optical and chemical sensors. *Nanomaterials* 2020;10:480. DOI PubMed PMC
12. Lim HR, Kim HS, Qazi R, Kwon YT, Jeong JW, Yeo WH. Advanced soft materials, sensor integrations, and applications of wearable flexible hybrid electronics in healthcare, energy, and environment. *Adv Mater* 2020;32:e1901924. DOI PubMed
13. Hua Q, Shen G. Low-dimensional nanostructures for monolithic 3D-integrated flexible and stretchable electronics. *Chem Soc Rev* 2024;53:1316-53. DOI PubMed
14. Wang Y, Haick H, Guo S, et al. Skin bioelectronics towards long-term, continuous health monitoring. *Chem Soc Rev* 2022;51:3759-93. DOI
15. Yang JC, Mun J, Kwon SY, Park S, Bao Z, Park S. Electronic skin: recent progress and future prospects for skin-attachable devices for health monitoring, robotics, and prosthetics. *Adv Mater* 2019;31:e1904765. DOI PubMed
16. Nie B, Liu S, Qu Q, Zhang Y, Zhao M, Liu J. Bio-inspired flexible electronics for smart E-skin. *Acta Biomater* 2022;139:280-95. DOI PubMed
17. Kim M, Kim S, Kwon YW, et al. Emerging bio-interfacing wearable devices for signal monitoring: overview of the mechanisms and diverse sensor designs to target distinct physiological bio-parameters. *Adv Sensor Res* 2023;2:2200049. DOI
18. Wu J, Chang L, Yu G. Effective data decision-making and transmission system based on mobile health for chronic disease management in the elderly. *IEEE Syst J* 2021;15:5537-48. DOI
19. Kichloo A, Albosta M, Dettloff K, et al. Telemedicine, the current COVID-19 pandemic and the future: a narrative review and perspectives moving forward in the USA. *Fam Med Community Health* 2020;8:e000530. DOI PubMed PMC
20. Moulaei K, Sheikhtaheri A, Fatehi F, Shanbehzadeh M, Bahaadinbeigy K. Patients' perspectives and preferences toward telemedicine versus in-person visits: a mixed-methods study on 1226 patients. *BMC Med Inform Decis Mak* 2023;23:261. DOI PubMed PMC
21. Jagadeeswari V, Subramaniyaswamy V, Logesh R, Vijayakumar V. A study on medical Internet of Things and Big Data in personalized healthcare system. *Health Inf Sci Syst* 2018;6:14. DOI PubMed PMC
22. Vaghasiya JV, Mayorga-Martinez CC, Pumera M. Wearable sensors for telehealth based on emerging materials and nanoarchitectonics. *Npj Flex Electron* 2023;7:26. DOI PubMed PMC
23. Ouyang X, Su R, Ng DWH, Han G, Pearson DR, McAlpine MC. 3D printed skin-interfaced UV-visible hybrid photodetectors. *Adv Sci* 2022;9:e2201275. DOI PubMed PMC
24. Lee HE, Lee D, Lee TI, et al. Siloxane hybrid material-encapsulated highly robust flexible μLEDs for biocompatible lighting applications. *ACS Appl Mater Interfaces* 2022;14:28258-69. DOI PubMed
25. Molina-Lopez F, Gao TZ, Kraft U, et al. Inkjet-printed stretchable and low voltage synaptic transistor array. *Nat Commun* 2019;10:2676. DOI PubMed PMC
26. Yang YJ, Cheng MY, Chang WY, et al. An integrated flexible temperature and tactile sensing array using PI-copper films. *Sensors Actuators A Phys* 2008;143:143-53. DOI
27. Ershad F, Thukral A, Yue J, et al. Ultra-conformal drawn-on-skin electronics for multifunctional motion artifact-free sensing and point-of-care treatment. *Nat Commun* 2020;11:3823. DOI PubMed PMC
28. Xu B, Akhtar A, Liu Y, et al. An epidermal stimulation and sensing platform for sensorimotor prosthetic control, management of lower back exertion, and electrical muscle activation. *Adv Mater* 2016;28:4462-71. DOI PubMed PMC
29. Lee GH, Kang H, Chung JW, et al. Stretchable PPG sensor with light polarization for physical activity-permissible monitoring. *Sci Adv* 2022;8:eabm3622. DOI PubMed PMC
30. Lee H, Song C, Baik S, Kim D, Hyeon T, Kim DH. Device-assisted transdermal drug delivery. *Adv Drug Deliv Rev* 2018;127:35-45. DOI
31. Choi S, Lee H, Ghaffari R, Hyeon T, Kim DH. Recent advances in flexible and stretchable bio-electronic devices integrated with nanomaterials. *Adv Mater* 2016;28:4203-18. DOI PubMed
32. Parrilla M, Detamornrat U, Domínguez-Robles J, Tunca S, Donnelly RF, De Wael K. Wearable microneedle-based array patches for continuous electrochemical monitoring and drug delivery: toward a closed-loop system for methotrexate treatment. *ACS Sens* 2023;8:4161-70. DOI
33. Yang J, Zheng S, Ma D, et al. Masticatory system-inspired microneedle theranostic platform for intelligent and precise diabetic management. *Sci Adv* 2022;8:eabo6900. DOI PubMed PMC
34. Chen W, Yan X. Progress in achieving high-performance piezoresistive and capacitive flexible pressure sensors: a review. *J Mater Sci Technol* 2020;43:175-88. DOI
35. Qin R, Nong J, Wang K, et al. Recent advances in flexible pressure sensors based on MXene materials. *Adv Mater* 2024;36:2312761. DOI
36. Eom J, Jaisutti R, Lee H, et al. Highly sensitive textile strain sensors and wireless user-interface devices using all-polymeric conducting fibers. *ACS Appl Mater Interfaces* 2017;9:10190-7. DOI
37. Wang C, Li X, Gao E, et al. Carbonized silk fabric for ultrastretchable, highly sensitive, and wearable strain sensors. *Adv Mater*

2016;28:6640-8. DOI PubMed
38. Zub K, Hoeppener S, Schubert US. Inkjet printing and 3D printing strategies for biosensing, analytical, and diagnostic applications. *Adv Mater* 2022;34:e2105015. DOI PubMed
39. Hempel M, Nezich D, Kong J, Hofmann M. A novel class of strain gauges based on layered percolative films of 2D materials. *Nano Lett* 2012;12:5714-8. DOI
40. Muth JT, Vogt DM, Truby RL, et al. Embedded 3D printing of strain sensors within highly stretchable elastomers. *Adv Mater* 2014;26:6307-12. DOI PubMed
41. Wang Y, Lee S, Yokota T, et al. A durable nanomesh on-skin strain gauge for natural skin motion monitoring with minimum mechanical constraints. *Sci Adv* 2020;6:eabb7043. DOI PubMed PMC
42. Liu K, Ouyang B, Guo X, Guo Y, Liu Y. Advances in flexible organic field-effect transistors and their applications for flexible electronics. *npj Flex Electron* 2022;6:1. DOI
43. So H, Sim JW, Kwon J, Yun J, Baik S, Chang WS. Carbon nanotube based pressure sensor for flexible electronics. *Mater Res Bull* 2013;48:5036-9. DOI
44. Fortunato E, Barquinha P, Martins R. Oxide semiconductor thin-film transistors: a review of recent advances. *Adv Mater* 2012;24:2945-86. DOI PubMed
45. Vigneshvar S, Sudhakumari CC, Senthilkumaran B, Prakash H. Recent advances in biosensor technology for potential applications - an overview. *Front Bioeng Biotechnol* 2016;4:11. DOI PubMed PMC
46. Kim DW, Min SY, Lee Y, Jeong U. Transparent flexible nanoline field-effect transistor array with high integration in a large area. *ACS Nano* 2020;14:907-18. DOI
47. Nela L, Tang J, Cao Q, Tulevski G, Han SJ. Large-area high-performance flexible pressure sensor with carbon nanotube active matrix for electronic skin. *Nano Lett* 2018;18:2054-9. DOI PubMed
48. Someya T, Kato Y, Sekitani T, et al. Conformable, flexible, large-area networks of pressure and thermal sensors with organic transistor active matrixes. *Proc Natl Acad Sci U S A* 2005;102:12321-5. DOI PubMed PMC
49. Kim KB, Baek HJ. Photoplethysmography in wearable devices: a comprehensive review of technological advances, current challenges, and future directions. *Electronics* 2023;12:2923. DOI
50. Lee HE, Kim S, Ko J, et al. Skin-like oxide thin-film transistors for transparent displays. *Adv Funct Mater* 2016;26:6170-8. DOI
51. Wang J, Zhang F, Zhang J, et al. Key issues and recent progress of high efficient organic light-emitting diodes. *J Photochem Photobiol C Photochem Rev* 2013;17:69-104. DOI
52. Jeon Y, Choi HR, Park KC, Choi KC. Flexible organic light-emitting-diode-based photonic skin for attachable phototherapeutics. *J Soc Inf Display* 2020;28:324-32. DOI
53. Kim TH, Lee CS, Kim S, et al. Fully stretchable optoelectronic sensors based on colloidal quantum dots for sensing photoplethysmographic signals. *ACS Nano* 2017;11:5992-6003. DOI
54. Yokota T, Zalar P, Kaltenbrunner M, et al. Ultraflexible organic photonic skin. *Sci Adv* 2016;2:e1501856. DOI PubMed PMC
55. Gillan L, Hiltunen J, Behfar MH, Rönkä K. Advances in design and manufacture of stretchable electronics. *Jpn J Appl Phys* 2022;61:SE0804. DOI
56. Lee HE, Lee D, Lee T, et al. Wireless powered wearable micro light-emitting diodes. *Nano Energy* 2019;55:454-62. DOI
57. Hu L, Choi J, Hwangbo S, et al. Flexible micro-LED display and its application in Gbps multi-channel visible light communication. *npj Flex Electron* 2022;6:100. DOI
58. Baeg K, Lee J. Flexible electronic systems on plastic substrates and textiles for smart wearable technologies. *Adv Mater Technol* 2020;5:2000071. DOI
59. Hassan M, Abbas G, Li N, et al. Significance of flexible substrates for wearable and implantable devices: recent advances and perspectives. *Adv Mater Technol* 2022;7:2100773. DOI
60. Someya T, Amagai M. Toward a new generation of smart skins. *Nat Biotechnol* 2019;37:382-8. DOI
61. Kim Y, Suh JM, Shin J, et al. Chip-less wireless electronic skins by remote epitaxial freestanding compound semiconductors. *Science* 2022;377:859-64. DOI
62. Kim JH, Park SY, Kim MK, et al. Long-term UV detecting wearable patches enabled by III-N compound semiconductor-based microphotodetectors. *Adv Opt Mater* 2023;11:2203083. DOI
63. Kim JH, Joe DJ, Lee HE. Sweat-permeable electronic skin with a pattern of eyes for body temperature monitoring. *Micro Nano Syst Lett* 2023;11:7. DOI
64. Yeon H, Lee H, Kim Y, et al. Long-term reliable physical health monitoring by sweat pore-inspired perforated electronic skins. *Sci Adv* 2021;7:eabg8459. DOI PubMed PMC
65. Xu C, Song Y, Han M, Zhang H. Portable and wearable self-powered systems based on emerging energy harvesting technology. *Microsyst Nanoeng* 2021;7:25. DOI PubMed PMC
66. Ali A, Shaukat H, Bibi S, Altabey WA, Noori M, Kouritem SA. Recent progress in energy harvesting systems for wearable technology. *Energy Strat Rev* 2023;49:101124. DOI
67. Islam E, Abdullah AM, Chowdhury AR, et al. Electromagnetic-triboelectric-hybrid energy tile for biomechanical green energy harvesting. *Nano Energy* 2020;77:105250. DOI
68. Wang H, Cheng J, Wang Z, Ji L, Wang Z. Triboelectric nanogenerators for human-health care. *Sci Bull* 2021;66:490-511. DOI
69. Niu S, Wang ZL. Theoretical systems of triboelectric nanogenerators. *Nano Energy* 2015;14:161-92. DOI

70. Gai Y, Wang E, Liu M, et al. A self-powered wearable sensor for continuous wireless sweat monitoring. *Small Methods* 2022;6:e2200653. DOI
71. Cheedarala RK, Song JI. Integrated electronic skin (e-skin) for harvesting of TENG energy through push-pull ionic electrets and ion-ion hopping mechanism. *Sci Rep* 2022;12:3879. DOI PubMed PMC
72. Liu X, Zhang Y, Wang X, et al. A battery-free wireless body area network towards state perception under all-weather conditions. *Nano Energy* 2023;116:108856. DOI
73. Samir A, Ashour FH, Hakim AAA, Bassyouni M. Recent advances in biodegradable polymers for sustainable applications. *npj Mater Degrad* 2022;6:68. DOI
74. Hosseini ES, Dervin S, Ganguly P, Dahiya R. Biodegradable materials for sustainable health monitoring devices. *ACS Appl Bio Mater* 2021;4:163-94. DOI PubMed PMC
75. Veeralingam S, Sahatiya P, Kadu A, Mattela V, Badhulika S. Direct, one-step growth of $NiSe_2$ on cellulose paper: a low-cost, flexible, and wearable with smartphone enabled multifunctional sensing platform for customized noninvasive personal healthcare monitoring. *ACS Appl Electron Mater* 2019;1:558-68. DOI
76. Wang L, Peng S, Patil A, Jiang J, Zhang Y, Chang C. Enzymatic crosslinked silk fibroin hydrogel for biodegradable electronic skin and pulse waveform measurements. *Biomacromolecules* 2022;23:3429-38. DOI
77. Torgbo S, Sukyai P. Biodegradation and thermal stability of bacterial cellulose as biomaterial: The relevance in biomedical applications. *Polym Degrad Stab* 2020;179:109232. DOI
78. Li Z, Gu X, Lou S, Zheng Y. The development of binary Mg-Ca alloys for use as biodegradable materials within bone. *Biomaterials* 2008;29:1329-44. DOI PubMed
79. Erdmann N, Angrisani N, Reifenrath J, et al. Biomechanical testing and degradation analysis of MgCa0.8 alloy screws: a comparative in vivo study in rabbits. *Acta Biomater* 2011;7:1421-8. DOI PubMed
80. Kang S, Hwang S, Yu S, et al. Biodegradable thin metal foils and spin-on glass materials for transient electronics. *Adv Funct Mater* 2015;25:1789-97. DOI
81. Paul SJ, Elizabeth I, Gupta BK. Ultrasensitive wearable strain sensors based on a VACNT/PDMS thin film for a wide range of human motion monitoring. *ACS Appl Mater Interfaces* 2021;13:8871-9. DOI PubMed
82. Hwang GT, Park H, Lee JH, et al. Self-powered cardiac pacemaker enabled by flexible single crystalline PMN-PT piezoelectric energy harvester. *Adv Mater* 2014;26:4880-7. DOI PubMed
83. Kim N, Chen J, Wang W, et al. Highly-sensitive skin-attachable eye-movement sensor using flexible nonhazardous piezoelectric thin film. *Adv Funct Mater* 2021;31:2008242. DOI
84. Yang T, Jiang X, Zhong Y, et al. A wearable and highly sensitive graphene strain sensor for precise home-based pulse wave monitoring. *ACS Sens* 2017;2:967-74. DOI
85. Currano LJ, Sage FC, Hagedon M, Hamilton L, Patrone J, Gerasopoulos K. Wearable sensor system for detection of lactate in sweat. *Sci Rep* 2018;8:15890. DOI PubMed PMC
86. Xu J, Tao X, Liu X, Yang L. Wearable eye patch biosensor for noninvasive and simultaneous detection of multiple biomarkers in human tears. *Anal Chem* 2022;94:8659-67. DOI
87. Bi Y, Sun M, Wang J, et al. Universal fully integrated wearable sensor arrays for the multiple electrolyte and metabolite monitoring in raw sweat, saliva, or urine. *Anal Chem* 2023;95:6690-9. DOI PubMed
88. Li S, Wang S, Wu B, et al. Unlocking pomegranate-structured wireless sensors with superhigh sensitivity via room-temperature water-driven rapid solidification of conductive pathways. *Nano Energy* 2024;120:109148. DOI
89. Kang BH, Park K, Hambsch M, et al. Skin-conformable photoplethysmogram sensors for energy-efficient always-on cardiovascular monitoring systems. *Nano Energy* 2022;92:106773. DOI
90. Wilkerson JE, Horvath SM, Gutin B, Molnar S, Diaz FJ. Plasma electrolyte content and concentration during treadmill exercise in humans. *J Appl Physiol Respir Environ Exerc Physiol* 1982;53:1529-39. DOI PubMed
91. Kellum JA. Determinants of blood pH in health and disease. *Crit Care* 2000;4:6-14. DOI PubMed PMC
92. Egi M, Bellomo R, Stachowski E, et al. Blood glucose concentration and outcome of critical illness: the impact of diabetes. *Crit Care Med* 2008;36:2249-55. DOI PubMed
93. Özbek O, Berkel C. Recent advances in potentiometric analysis: paper-based devices. *Sensors Int* 2022;3:100189. DOI
94. Parrilla M, Cuartero M, Crespo GA. Wearable potentiometric ion sensors. *TrAC Trends Anal Chem* 2019;110:303-20. DOI
95. Criscuolo F, Ny Hanitra I, Aiassa S, et al. Wearable multifunctional sweat-sensing system for efficient healthcare monitoring. *Sensors Actuators B Chem* 2021;328:129017. DOI
96. Sharma A, Ansari MZ, Cho C. Ultrasensitive flexible wearable pressure/strain sensors: Parameters, materials, mechanisms and applications. *Sensors Actuators A Phys* 2022;347:113934. DOI
97. Li X, Zhang R, Yu W, et al. Stretchable and highly sensitive graphene-on-polymer strain sensors. *Sci Rep* 2012;2:870. DOI PubMed PMC
98. Xiao X, Yuan L, Zhong J, et al. High-strain sensors based on ZnO nanowire/polystyrene hybridized flexible films. *Adv Mater* 2011;23:5440-4. DOI PubMed
99. Teng F, Zi T, Fang J, Liu C, Wu D, Li A. Extremely sensitive wearable strain sensor with wide range based on a simple parallel connection architecture. *Adv Elect Mater* 2023;9:2200993. DOI
100. Kim SR, Kim JH, Park JW. Wearable and transparent capacitive strain sensor with high sensitivity based on patterned ag nanowire

networks. *ACS Appl Mater Interfaces* 2017;9:26407-16. DOI PubMed

101. Hardman D, George Thuruthel T, Iida F. Self-healing ionic gelatin/glycerol hydrogels for strain sensing applications. *NPG Asia Mater* 2022;14:11. DOI
102. Tolvanen J, Hannu J, Jantunen H. Stretchable and washable strain sensor based on cracking structure for human motion monitoring. *Sci Rep* 2018;8:13241. DOI PubMed PMC
103. Acott TS, Kelley MJ. Extracellular matrix in the trabecular meshwork. *Exp Eye Res* 2008;86:543-61. DOI PubMed PMC
104. Johnson M. 'What controls aqueous humour outflow resistance?'. *Exp Eye Res* 2006;82:545-57. DOI PubMed PMC
105. Medeiros FA, Weinreb RN, Zangwill LM, et al. Long-term intraocular pressure fluctuations and risk of conversion from ocular hypertension to glaucoma. *Ophthalmology* 2008;115:934-40. DOI PubMed PMC
106. Liu X, Ye Y, Ge Y, et al. Smart contact lenses for healthcare monitoring and therapy. *ACS Nano* 2024;18:6817-44. DOI
107. Seo H, Chung WG, Kwon YW, et al. Smart contact lenses as wearable ophthalmic devices for disease monitoring and health management. *Chem Rev* 2023;123:11488-558. DOI PubMed PMC
108. Kim TY, Mok JW, Hong SH, et al. Wireless theranostic smart contact lens for monitoring and control of intraocular pressure in glaucoma. *Nat Commun* 2022;13:6801. DOI PubMed PMC
109. Tseng P, Napier B, Garbarini L, Kaplan DL, Omenetto FG. Functional, RF-trilayer sensors for tooth-mounted, wireless monitoring of the oral cavity and food consumption. *Adv Mater* 2018;30:e1703257. DOI PubMed
110. Gloede ME, Paulauskas EE, Gregg MK. Experience and information loss in auditory and visual memory. *Q J Exp Psychol* 2017;70:1344-52. DOI PubMed
111. Hong SY, Kim MS, Park H, et al. High-sensitivity, skin-attachable, and stretchable array of thermo-responsive suspended gate field-effect transistors with thermochromic display. *Adv Funct Mater* 2019;29:1807679. DOI
112. Chun KS, Kang YJ, Lee JY, et al. A skin-conformable wireless sensor to objectively quantify symptoms of pruritus. *Sci Adv* 2021;7:eabf9405. DOI PubMed PMC
113. Rambwawasvika H. Alopecia types, current and future treatment. *J Dermat Cosmetol* 2021;5:93-9. DOI
114. Yoo KH, Kim MN, Kim BJ, Kim CW. Treatment of alopecia areata with fractional photothermolysis laser. *Int J Dermatol* 2010;49:845-7. DOI PubMed
115. Perper M, Aldahan AS, Fayne RA, Emerson CP, Nouri K. Efficacy of fractional lasers in treating alopecia: a literature review. *Lasers Med Sci* 2017;32:1919-25. DOI PubMed
116. Lee HE, Lee SH, Jeong M, et al. Trichogenic photostimulation using monolithic flexible vertical AlGaInP light-emitting diodes. *ACS Nano* 2018;12:9587-95. DOI
117. Joo H, Lee Y, Kim J, et al. Soft implantable drug delivery device integrated wirelessly with wearable devices to treat fatal seizures. *Sci Adv* 2021;7:eabd4639. DOI PubMed PMC
118. Wang C, Jiang X, Kim HJ, et al. Flexible patch with printable and antibacterial conductive hydrogel electrodes for accelerated wound healing. *Biomaterials* 2022;285:121479. DOI
119. Lee JH, Ahn Y, Lee HE, et al. Wearable surface-lighting micro-light-emitting diode patch for melanogenesis inhibition. *Adv Healthc Mater* 2023;12:e2201796. DOI PubMed
120. Ouyang Z, Li S, Liu J, et al. Bottom-up reconstruction of smart textiles with hierarchical structures to assemble versatile wearable devices for multiple signals monitoring. *Nano Energy* 2022;104:107963. DOI